Numerical simulation of cosmic ray protons over time measured by AMS-02

V. Bindi, C. Consolandi, **C. Corti**,
C. Light, M. Palermo, A. Popkov, K. Whitman
University of Hawaii

Washington DC, Apr 26th, 2017

Outline

- New parametrization for the proton LIS based on Voyager 1 and AMS-02
- Numerical model for GCR transport in the heliosphere
- Fitting procedure on AMS-02 monthly proton fluxes
- Results

Voyager 1

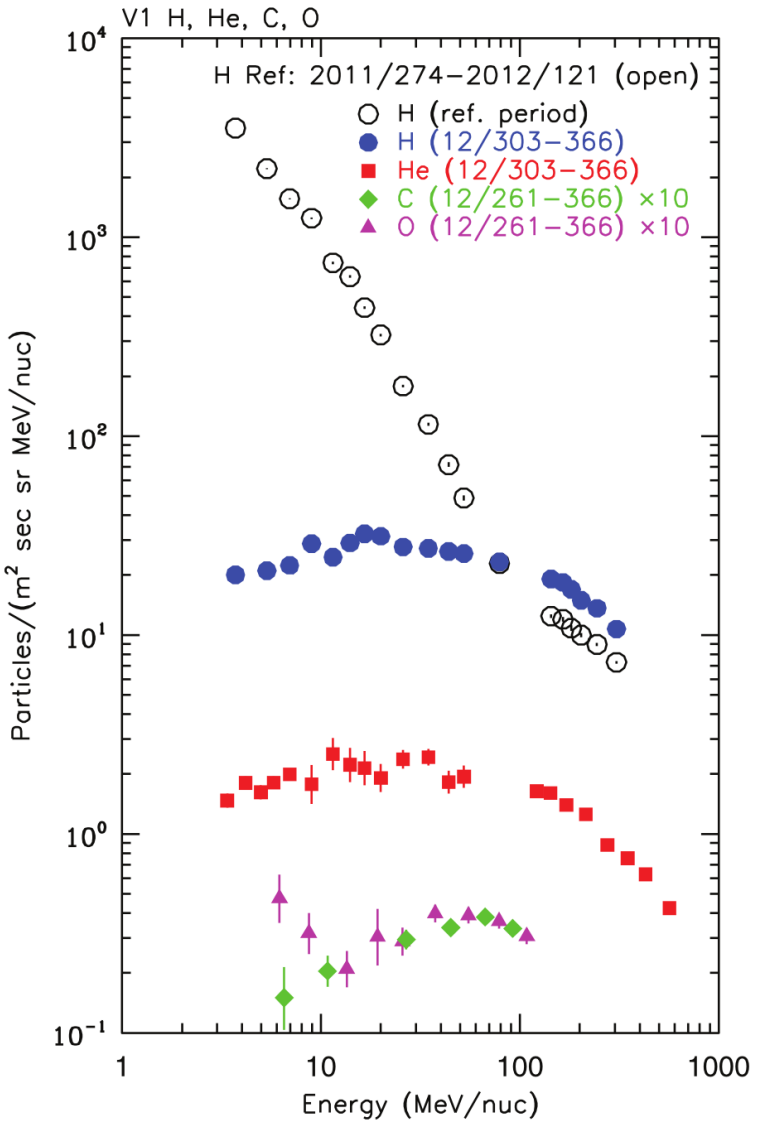

- 25 August 2012: Voyager 1 reaches the heliopause (caveat)
- Fluxes stable since then: best candidate for low energy range of the local interstellar spectrum (LIS)

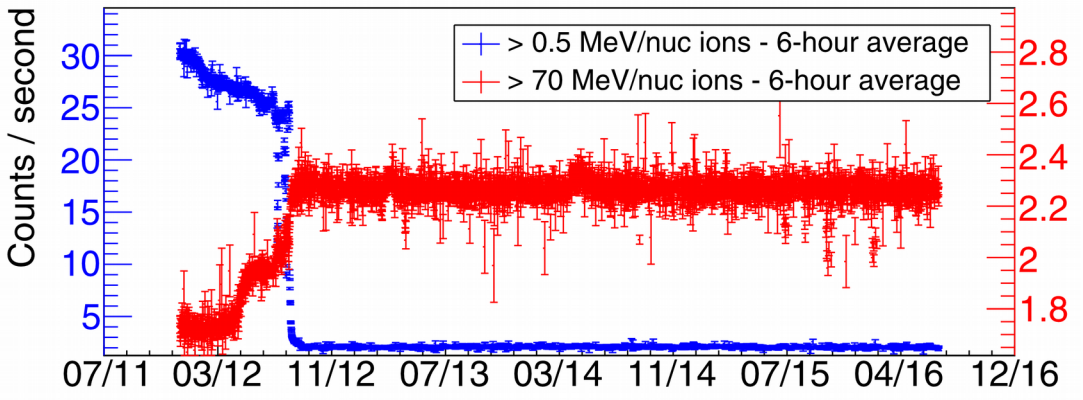

AMS-02 proton flux

- Proton flux May 2011 - November 2013: PRL 114 (2015)
  Smooth change of slope around 300 GV
  Best candidate for the high energy range of the LIS

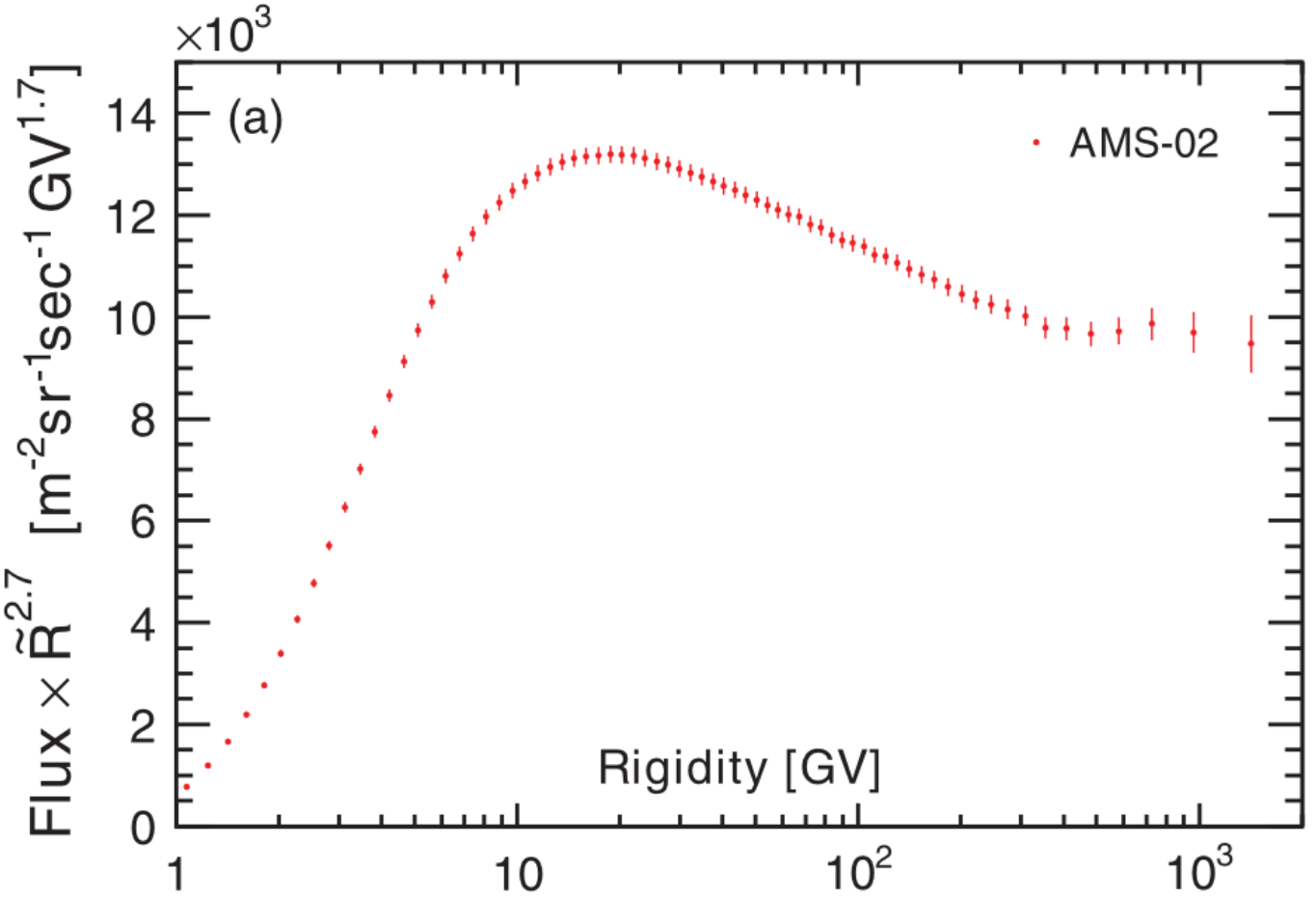

New LIS parametrization

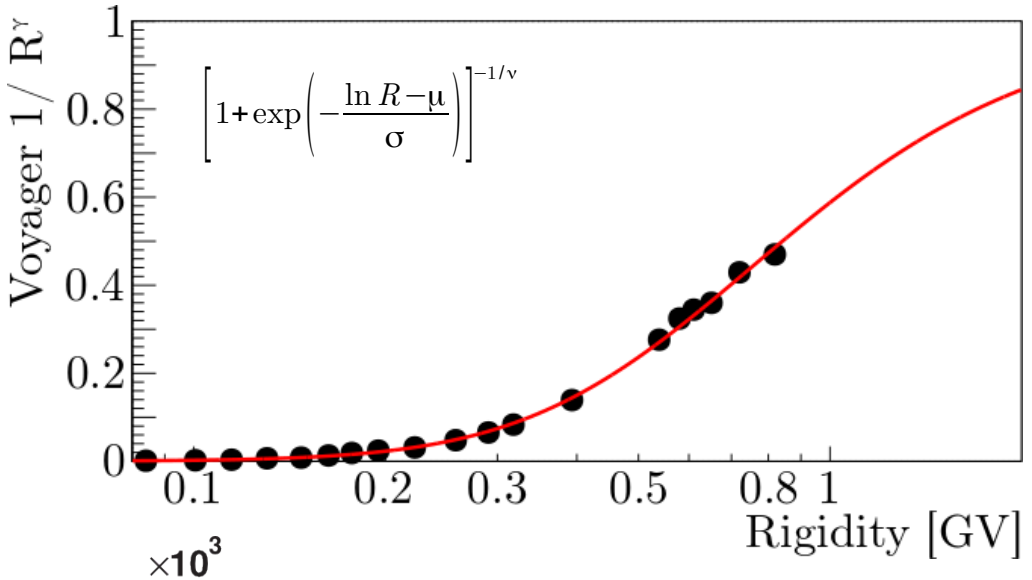

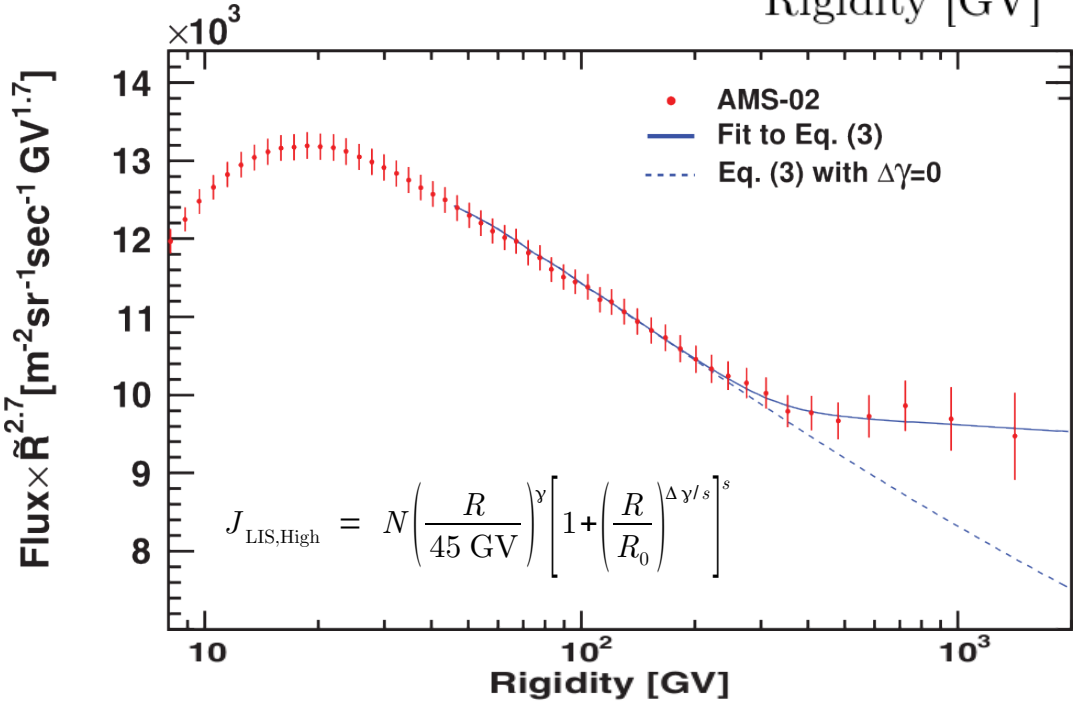

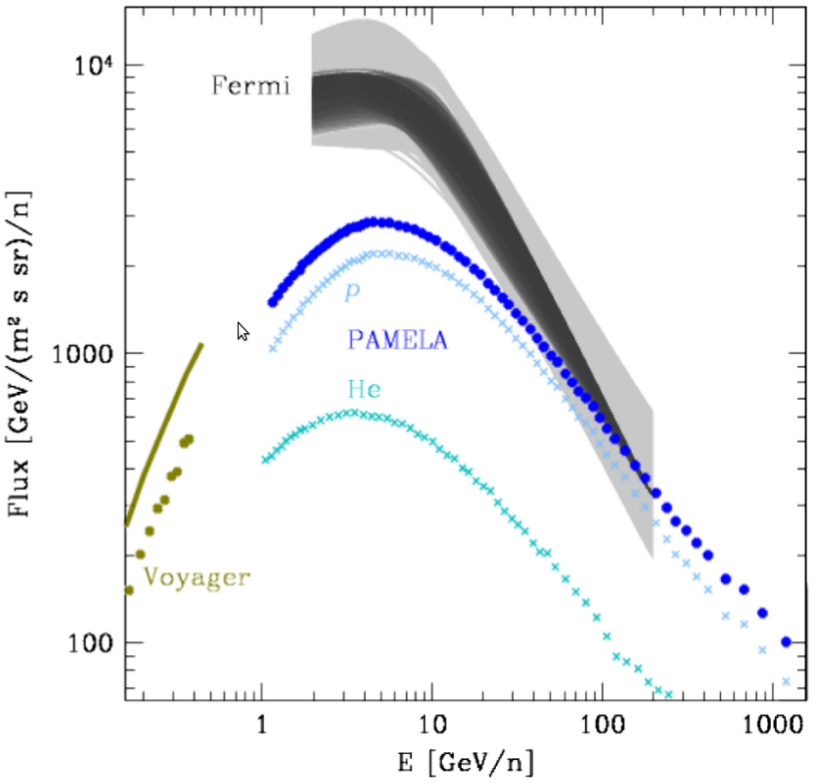

New LIS parametrization

$$\frac{\mathrm{d}\,J_{LIS}}{\mathrm{d}\,R}(R) \;=\; N \left[1 + \exp\left(-\frac{\ln R - \mu}{\sigma}\right)\right]^{-1/\nu} R^{\gamma_1} \left\{1 + \left[\frac{R}{R_{b1}}\left(1 + \left(\frac{R}{R_{b2}}\right)^{\frac{\Delta\gamma_2}{s_2}}\right)^{s_2}\right]^{\frac{\Delta\gamma_1}{s_1}}\right\}^{s_1}$$

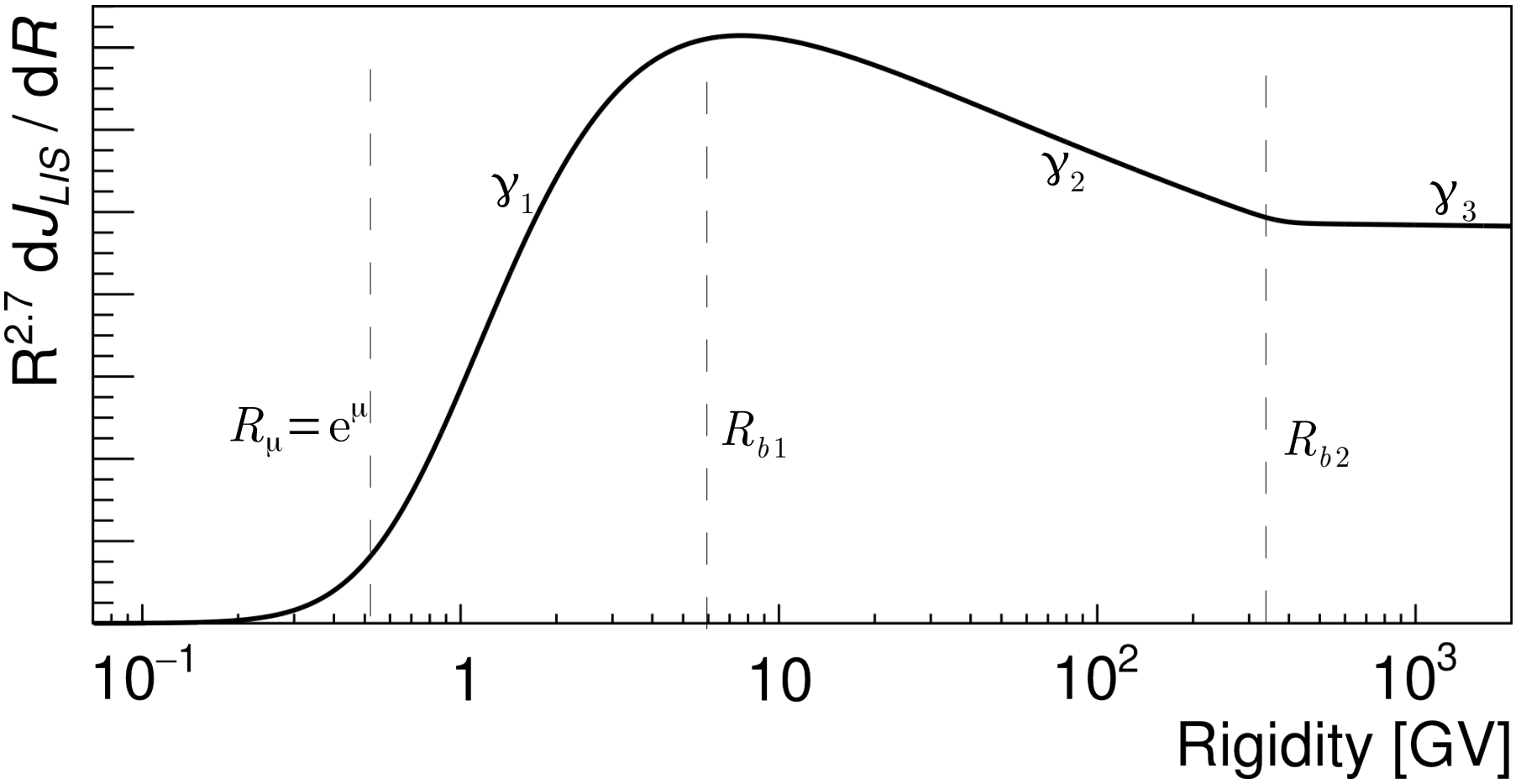

LIS fit on Voyager 1 and AMS-02

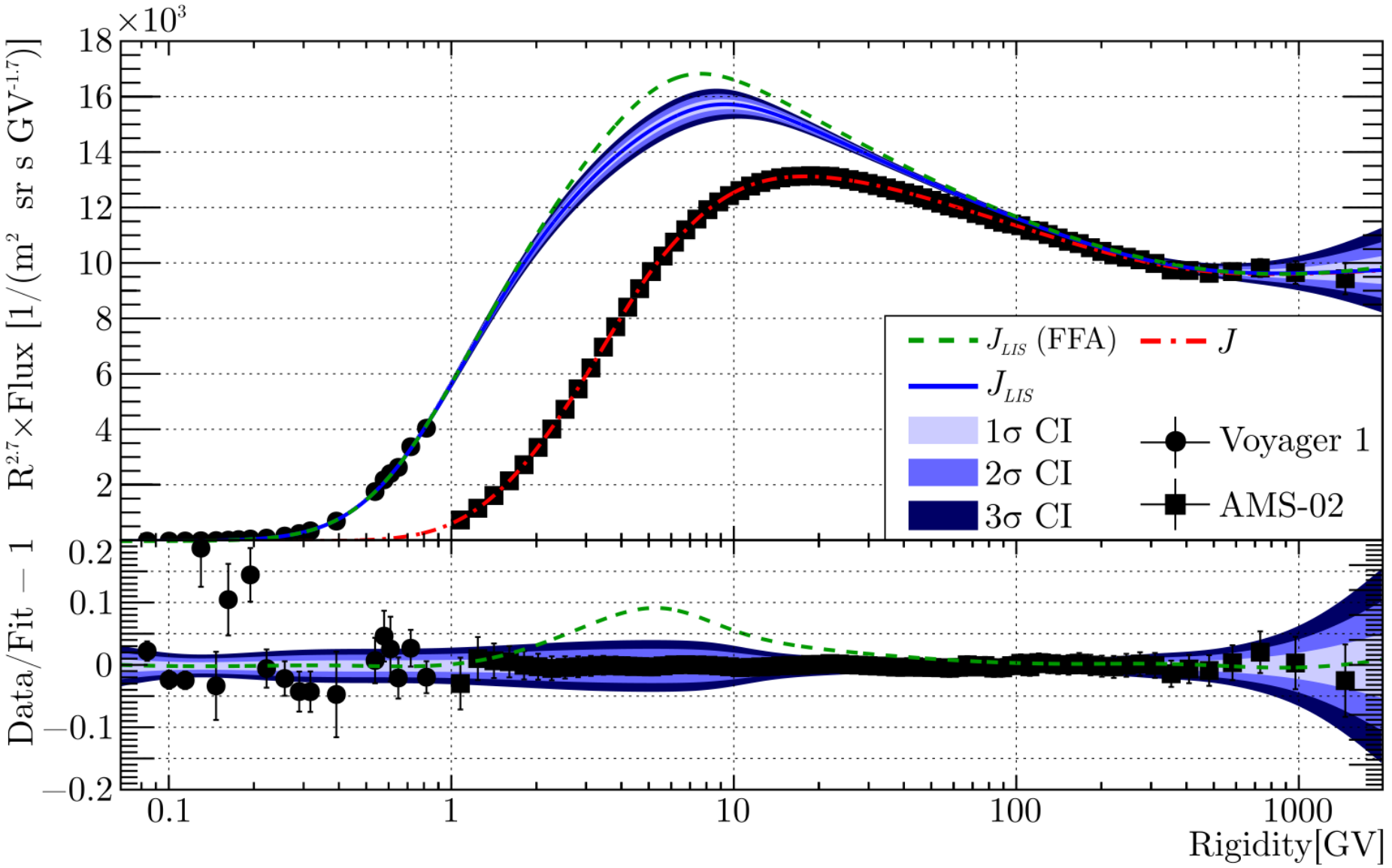

Explaining AMS-02 monthly fluxes

A three-dimensional numerical model for solving the Parker equation has been tuned to match the AMS-02 proton monthly fluxes during the maximum of solar cycle 24

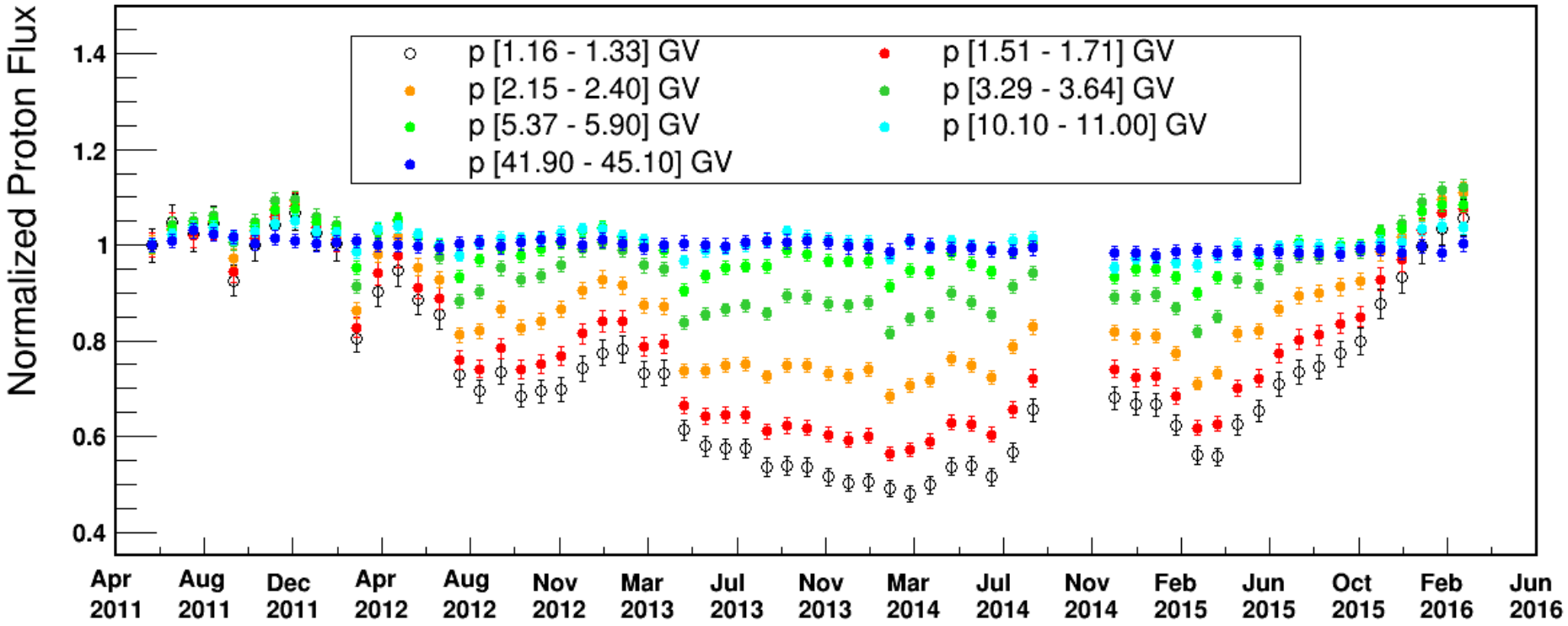

Transport equation of GCRs

GCR propagation in the heliosphere is described by the Parker equation:

$$\frac{\partial f}{\partial t} = \underbrace{-\vec{V}_{SW}\cdot\vec{\nabla} f}_{\text{Solar wind plasma convection}} \underbrace{-\vec{V}_{D}\cdot\vec{\nabla} f}_{\text{Particle drift}} + \underbrace{\vec{\nabla}\cdot\left(K\cdot\vec{\nabla} f\right)}_{\text{Particle diffusion}} + \underbrace{\frac{1}{3}\vec{\nabla}\cdot\vec{V}_{SW}\frac{\partial f}{\partial \ln R}}_{\text{Energy losses}} + \underbrace{Q}_{\text{Sources/ sinks}}$$

K = diffusion tensor
f = omnidirectional distribution function of GCRs

Particle drifts due to heliospheric magnetic field gradients and heliospheric current sheet.

Adiabatic energy losses due to expansion of solar wind.

It does not describe possible acceleration at the termination shock or short time-scale phenomena.

Numerical model description

- Created in South Africa (Burger, Potgieter) in FORTRAN (1998), then translated in C (2010) and C++/ROOT (2016)
- Three-dimensional steady-state model solving numerically the Parker transport equation of galactic cosmic rays in the heliosphere with the ADI (Alternating Direction Implicit) method
- Nvidia CUDA (2010) and OpenMP (2017) support to run in parallel
- Input: LIS, tilt angle, solar wind speed and IMF @ Earth, diffusion and drift coefficients
- Output: modulated flux at all grid positions in the heliosphere

Solar wind speed

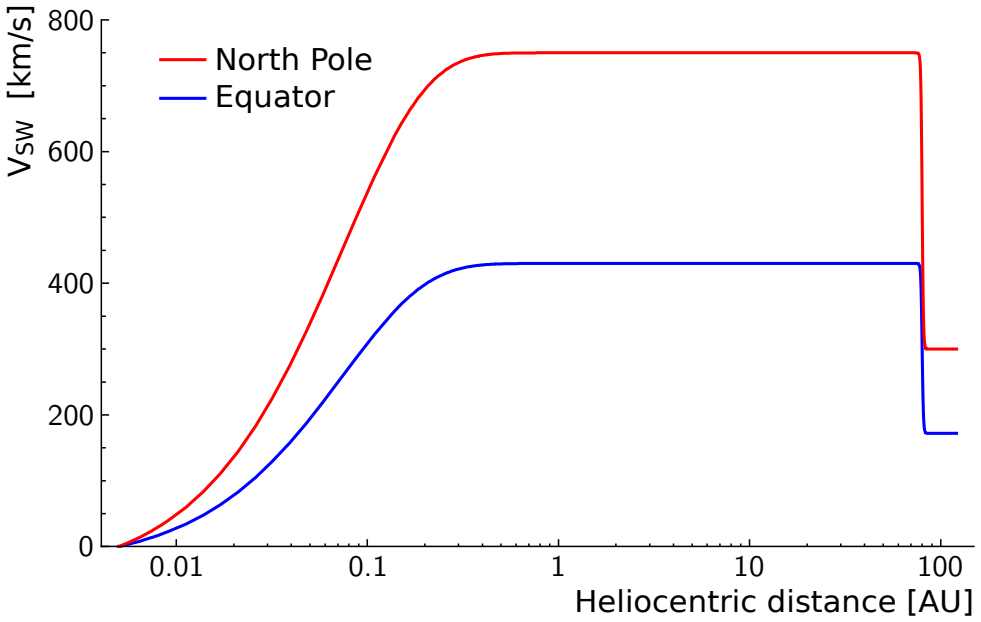

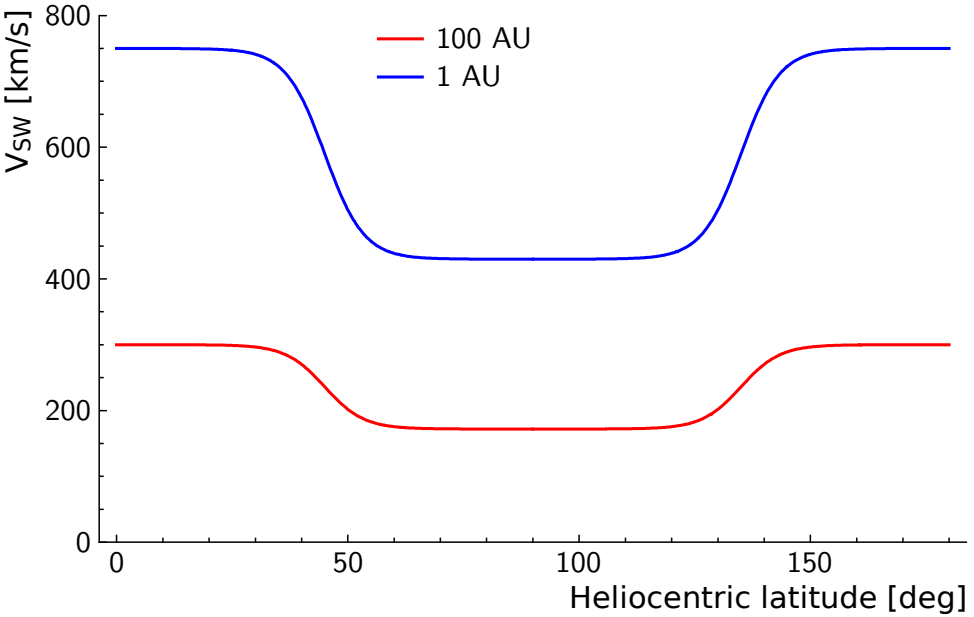

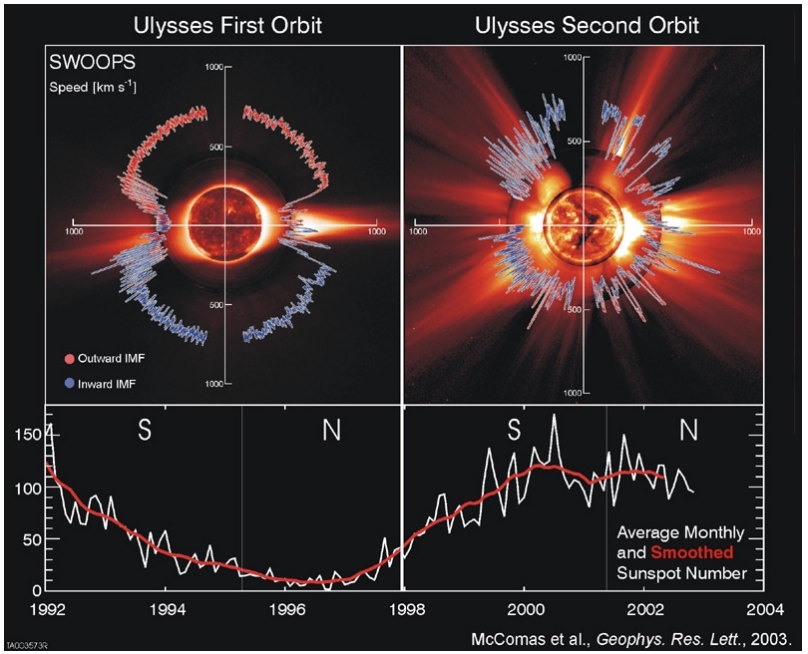

During the maximum, is essentially flat with latitude, but highly variable.
Assume same velocity at the Equator and at the Poles

Heliospheric magnetic field

Parker field

$$\vec{B} = A\, B_0 \left(\frac{r_0}{r}\right)^2 \left[\hat{r} + \frac{\omega\,(r-b)}{v}\sin\theta\,\hat{\phi}\right] \underbrace{\left[1 - 2\,H\,(\theta - \theta_{HCS})\right]}$$

Polarity

Current sheet

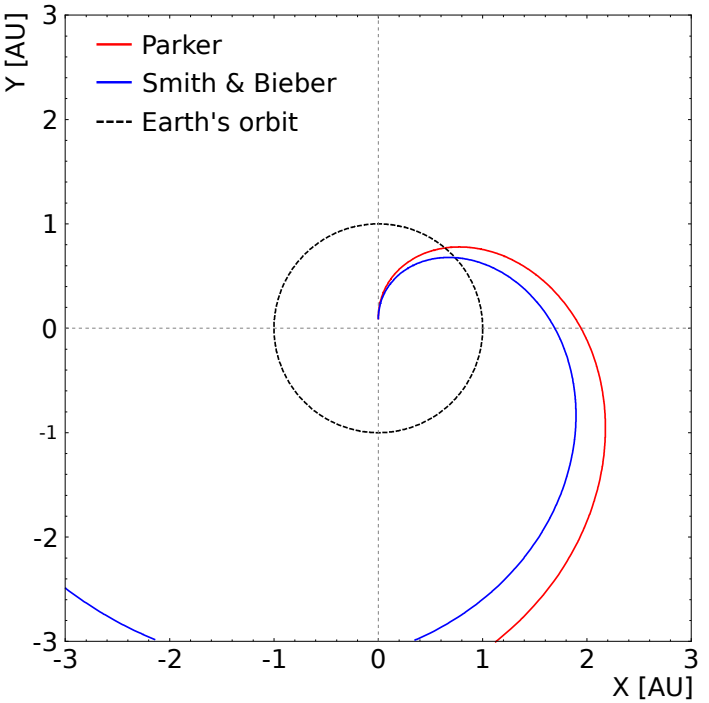

Smith-Bieber modification

Slightly larger spiral angle to match observations, due to the differential rotation of the Sun which induces a non-zero azimuthal component in the reference frame of the Sun.

$$\tan\psi = -B_\phi / B_r = \frac{\omega\,(r-b)}{V_{SW}(r,\theta)}\sin\theta - \frac{r}{b}\,\frac{V_{SW}(b,\theta)}{V_{SW}(r,\theta)}\,\frac{B_T(b)}{B_R(b)}$$

with $b = 20\,R_{Sun}$ and $\delta_{SB} = \dfrac{B_T(b)}{B_R(b)} = -0.02$

Diffusion and drift coefficients

Parallel diffusion

$$\kappa_{\parallel} = \frac{v^2}{8}\int_{-1}^{1}\frac{(1-\mu^2)^2}{\Phi(\mu)}d\mu$$

Rate of particle scattering, from the power spectrum of magnetic fluctuations

6x10^{20} cm^2 s^{-1}

Parametrization: $k_{\parallel} = k_{\parallel,0}\,\beta\,\frac{B_0}{B}\left(\frac{P}{P_k}\right)^a\left[1+\left(\frac{P}{P_k}\right)^{\frac{b-a}{c}}\right]^c$

Spatial dependence

Rigidity dependence

Perpendicular diffusion

$$\kappa_{\perp,r} = \kappa^0_{\perp,r}\kappa_{\parallel}$$ 2%

$$\kappa_{\perp,\theta} = f(\theta)\kappa^0_{\perp,\theta}\kappa_{\parallel}$$ 1%

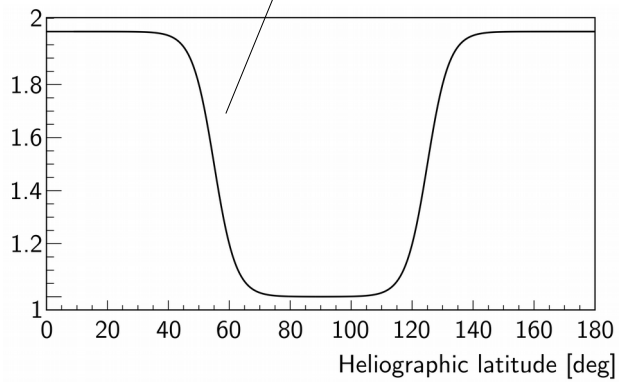

Drifts

$$\langle \mathbf{v}_A \rangle = \frac{pv}{3q}\frac{(\omega\tau_A)^2}{1+(\omega\tau_A)^2}\nabla\times\frac{\mathbf{B}}{B^2} = \nabla\times\kappa_A\mathbf{e}_B$$

$$\kappa_A = \kappa_{A,0}\frac{v}{3}r_L\frac{\left(\frac{P}{P_{A,0}}\right)^2}{1+\left(\frac{P}{P_{A,0}}\right)^2}$$

Scattering correction

Weak scattering limit

$r_L = P/B$

Model instability

Due to numerical errors, some set of parameters cause the model to become unstable: the solution oscillates with high frequency and can be even negative or infinite.

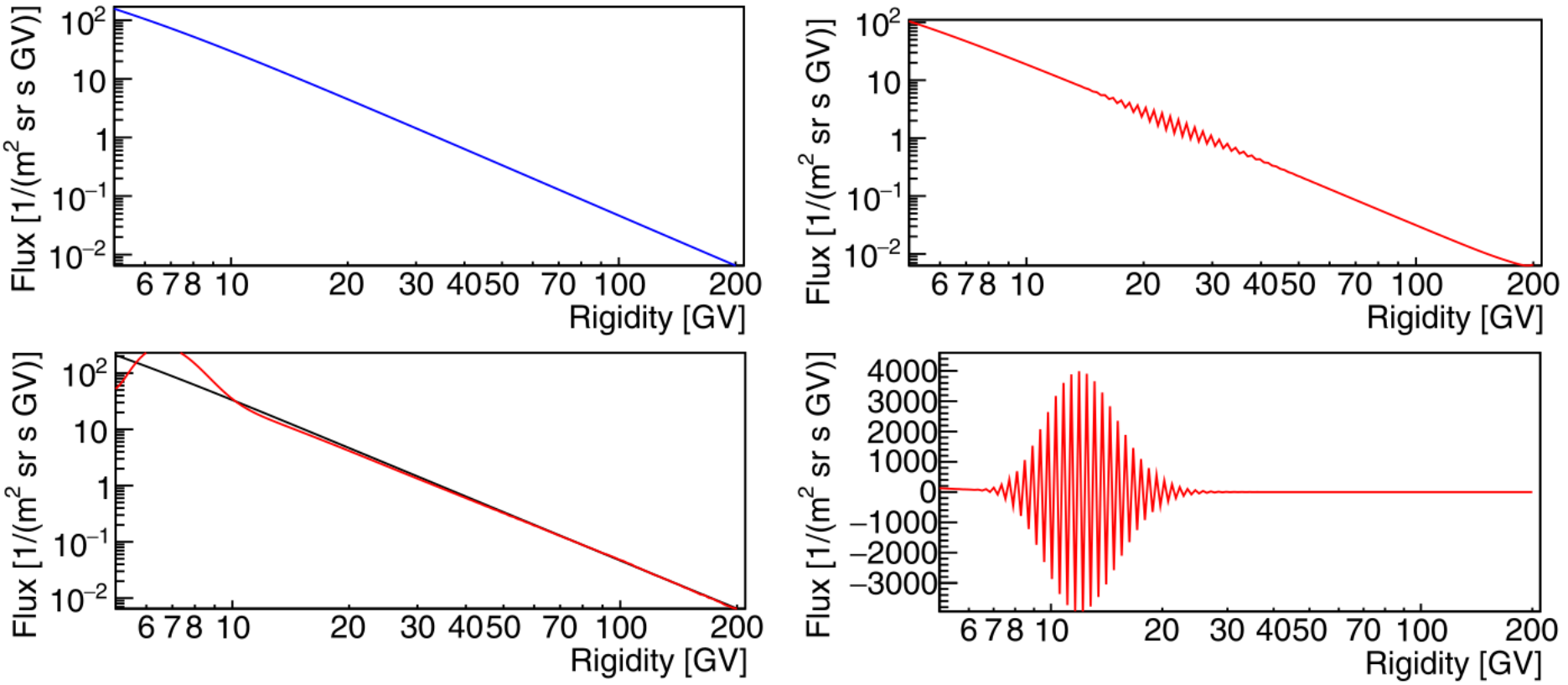

Model instability

Models with positive polarity fail less: protons enter from the poles and spend less time in the current sheet.

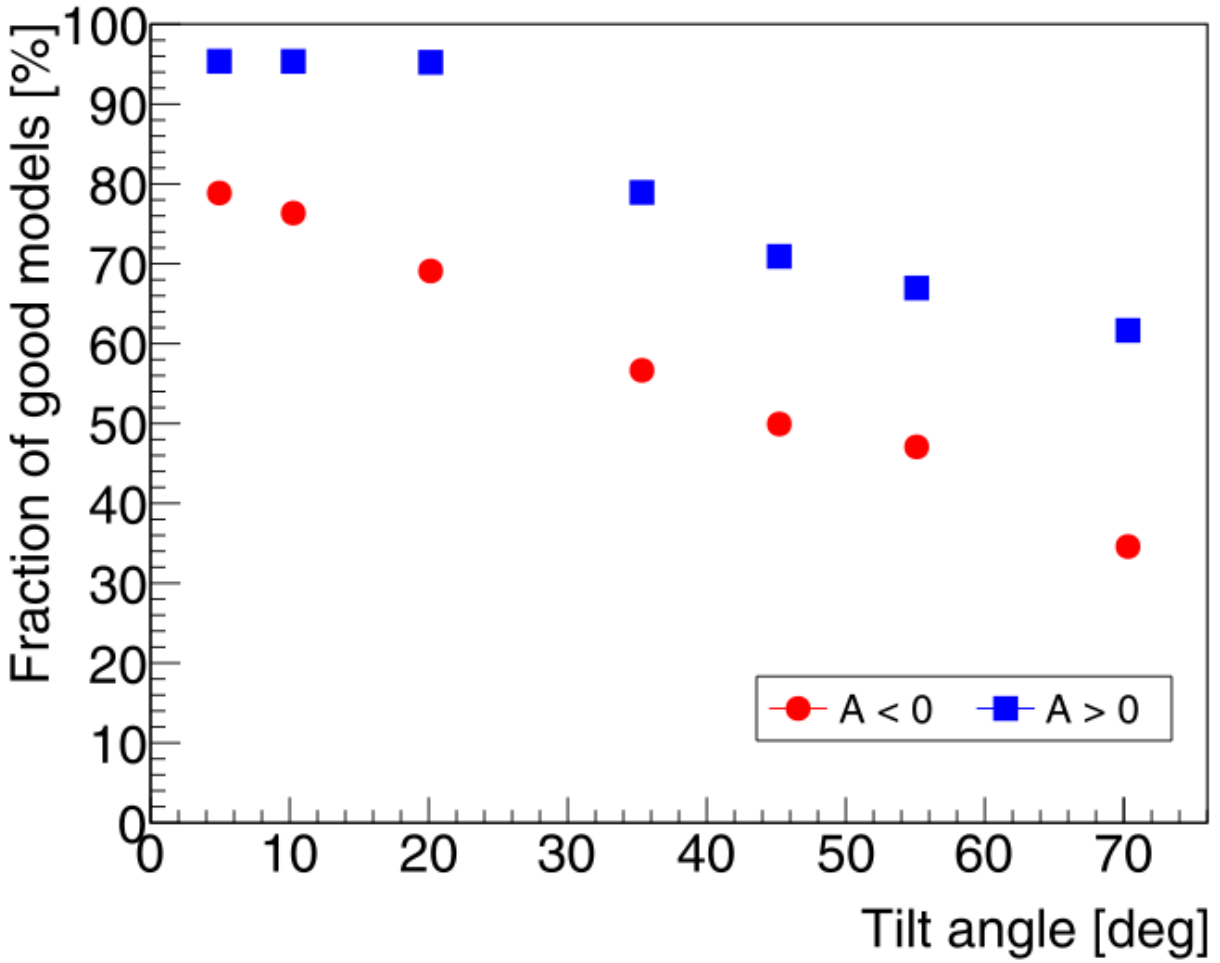

Models generatiom

- Grid scansion in 8-parameters space: $\simeq$ 1.6 million models
  - tilt angle α, magnetic field strength B_0 and polarity A
  - DC normalization $k_{\parallel 0}$
  - parallel DC slopes $a_{\parallel}$ and $b_{\parallel}$
  - perpendicular DC slopes, $a_{\perp r} < a_{\parallel}$ and $b_{\perp r} < b_{\parallel}$
- Rigidity grid: $1 - 200$ GV
- DC change of slope fixed at $P_k = 4.3$ GV
- Drift scattering correction fixed at $P_{A0} = 0.55$ GV
- Termination shock $= 80$ AU, Heliopause $= 122$ AU

Fitting procedure

- Earth position fixed at $\mathrm{r} = 1\ \mathrm{AU}$, $\theta = 90°$, $\varphi = 0°$

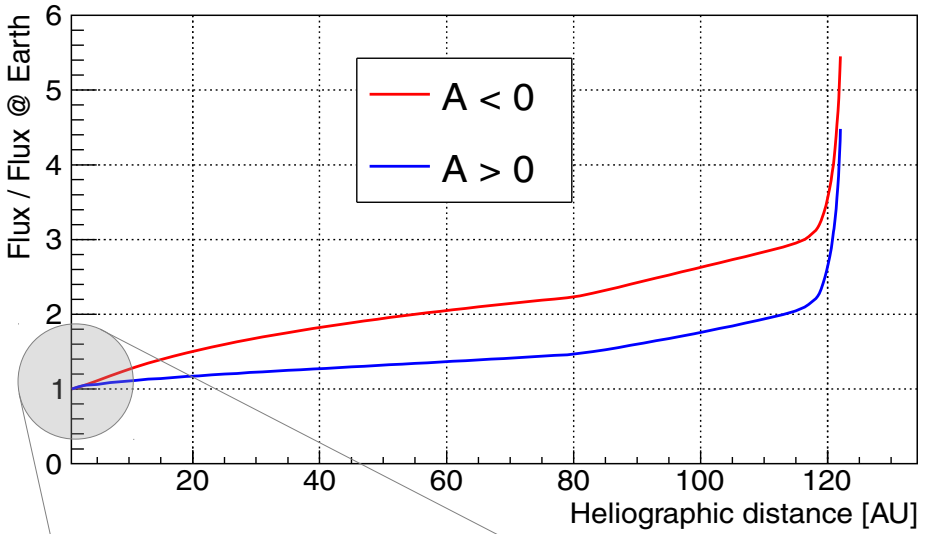

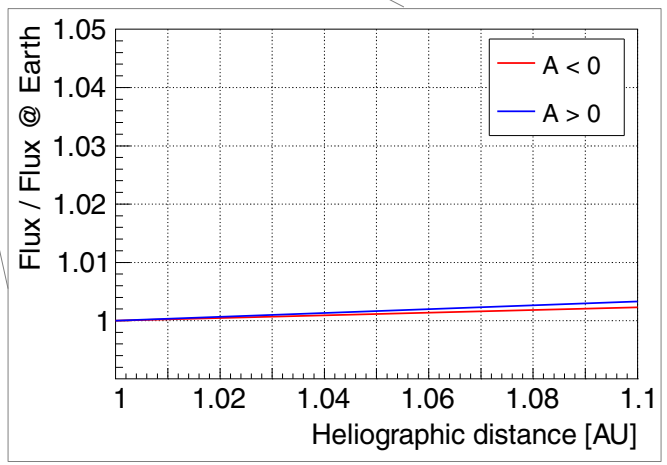

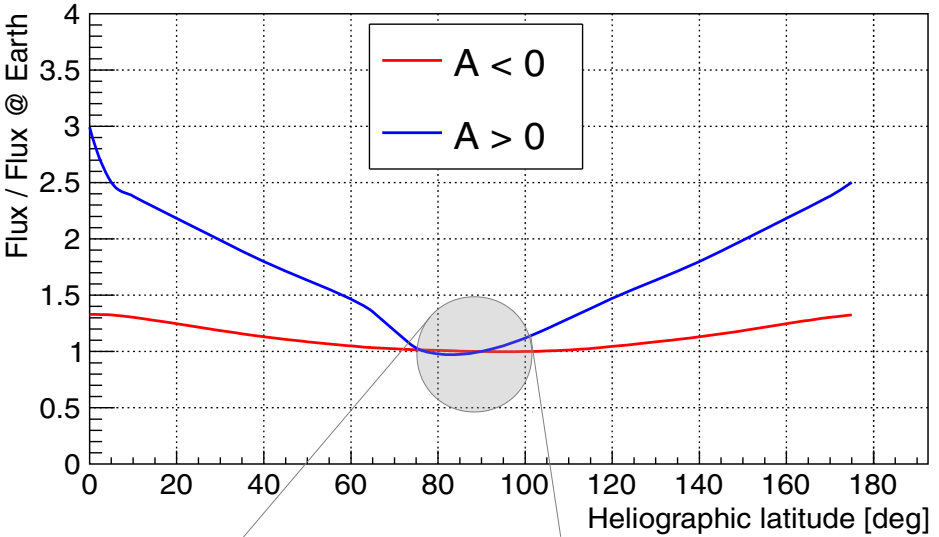

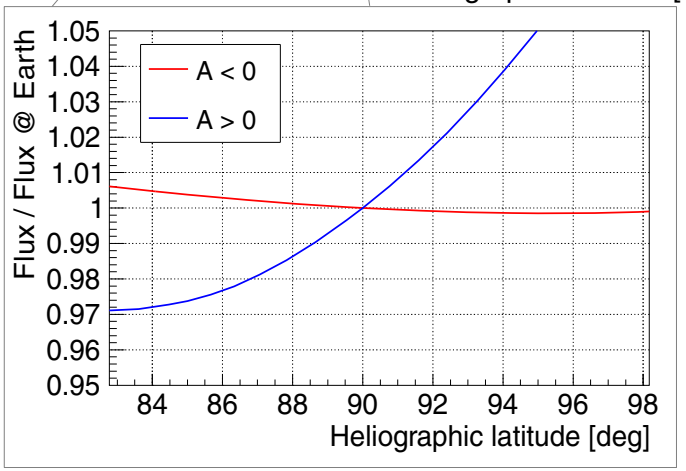

Fitting procedure

- For each AMS-02 monthly flux, fix the tilt angle and the magnetic field strength to the average value of the preceding 12 months

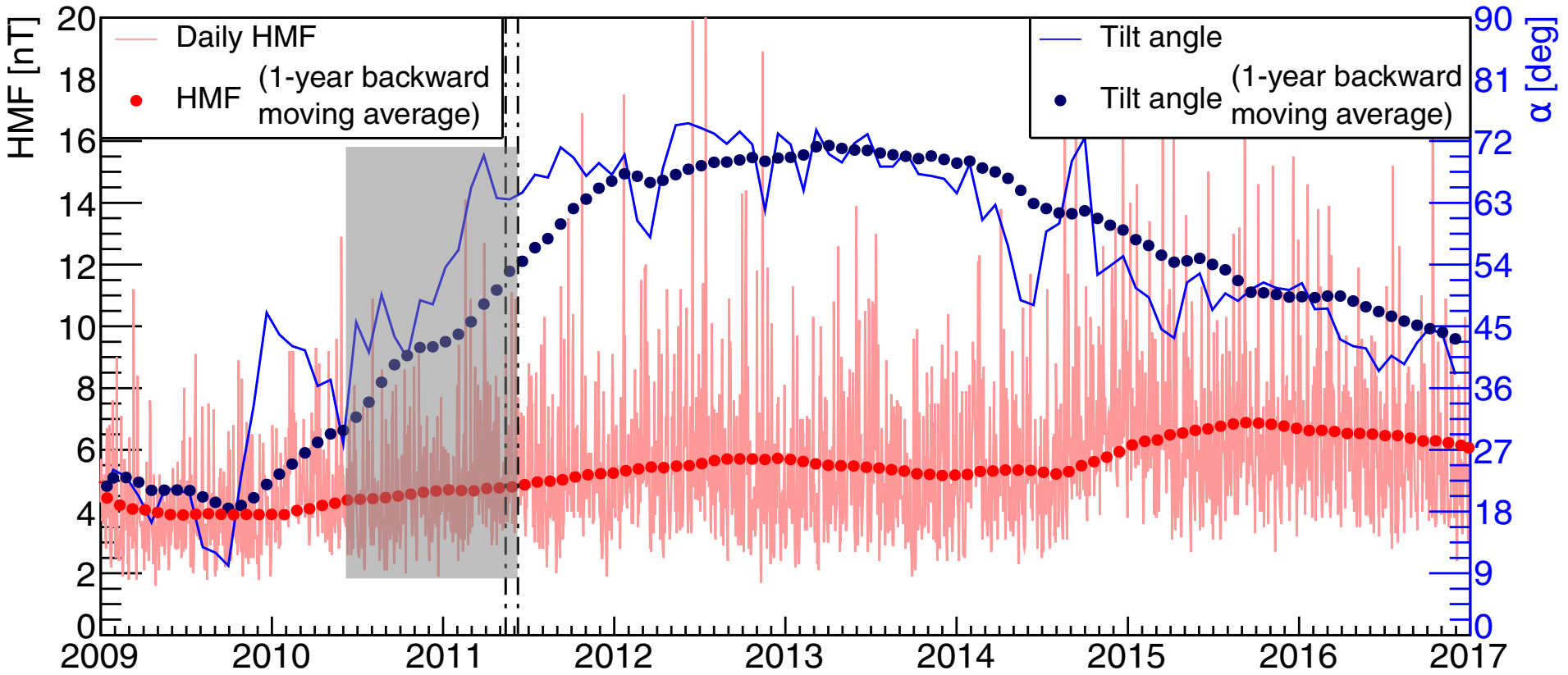

Fitting procedure

- Interpolate the simulated fluxes for a given tilt angle and magnetic field strength

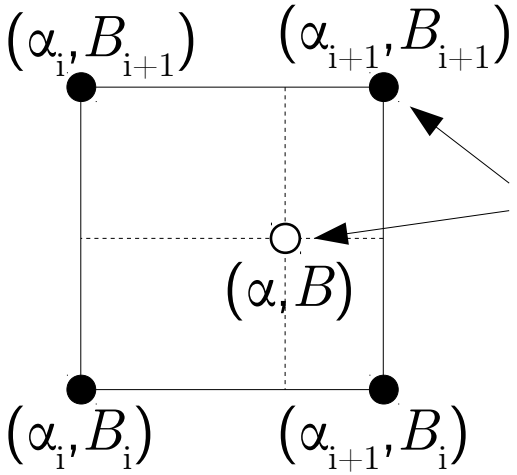

Each dot is a collection of models with fixed α, B and varying DC parameters.

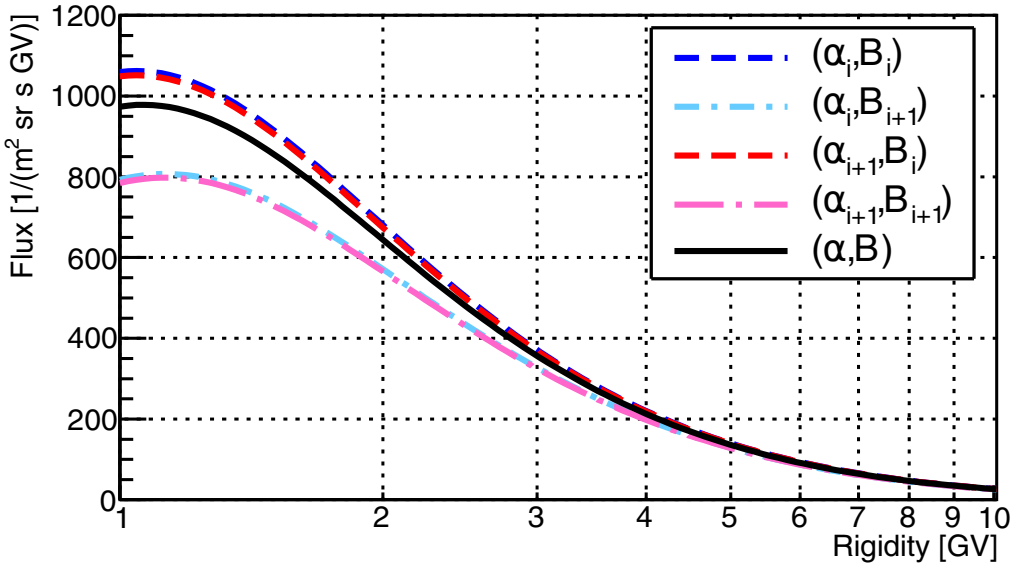

- For each AMS-02 monthly flux, compute the chi-squared between data and every model

Model uncertainty

Weighting each model by its likelihood ($e^{-\chi^2/2}$) allows the estimation of the model uncertainty.

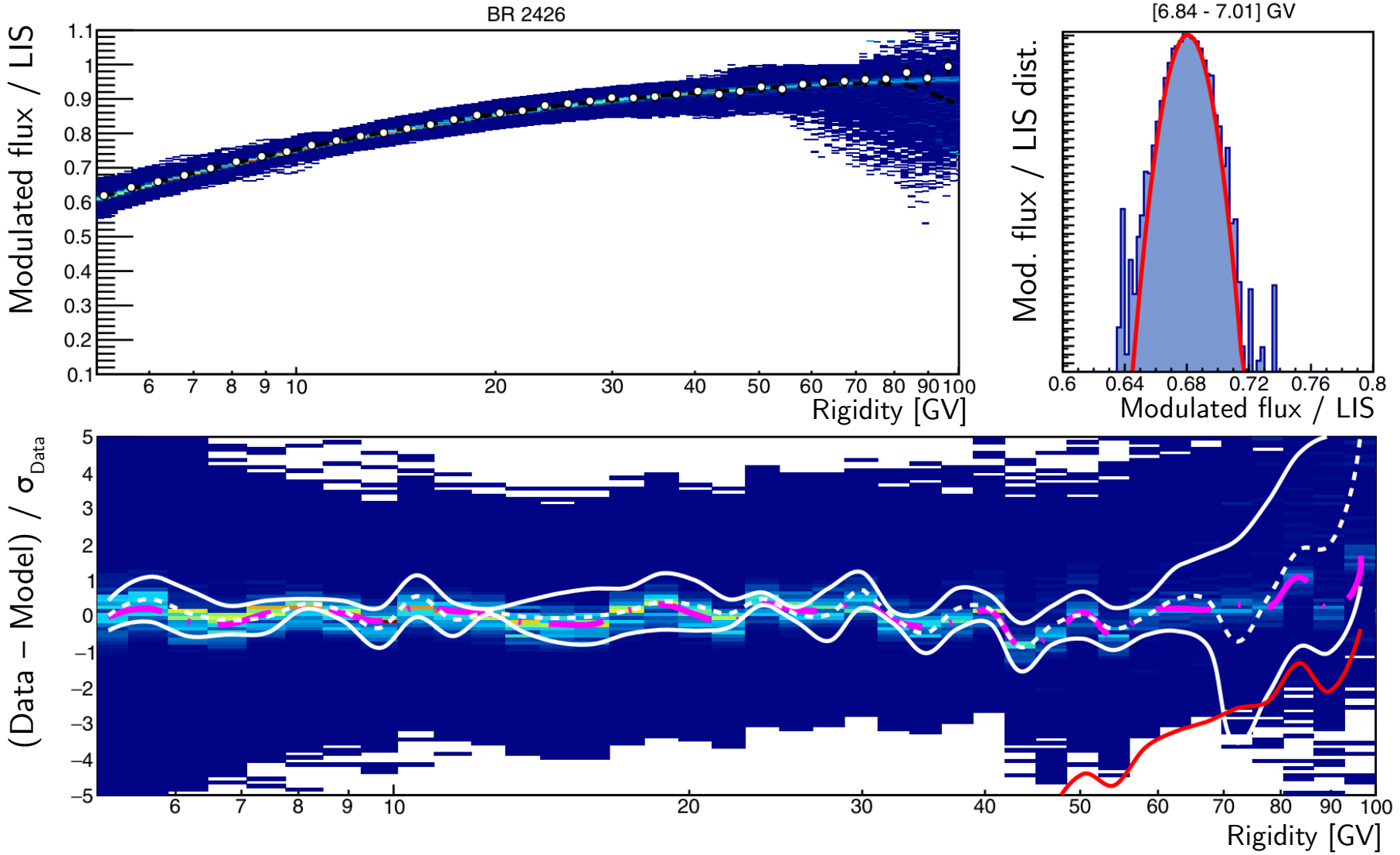

Best-fit parameter estimation

For each parameter, marginalize over the other parameters to plot chi-squared vs parameter and get the best-fit parameters with the uncertainty.

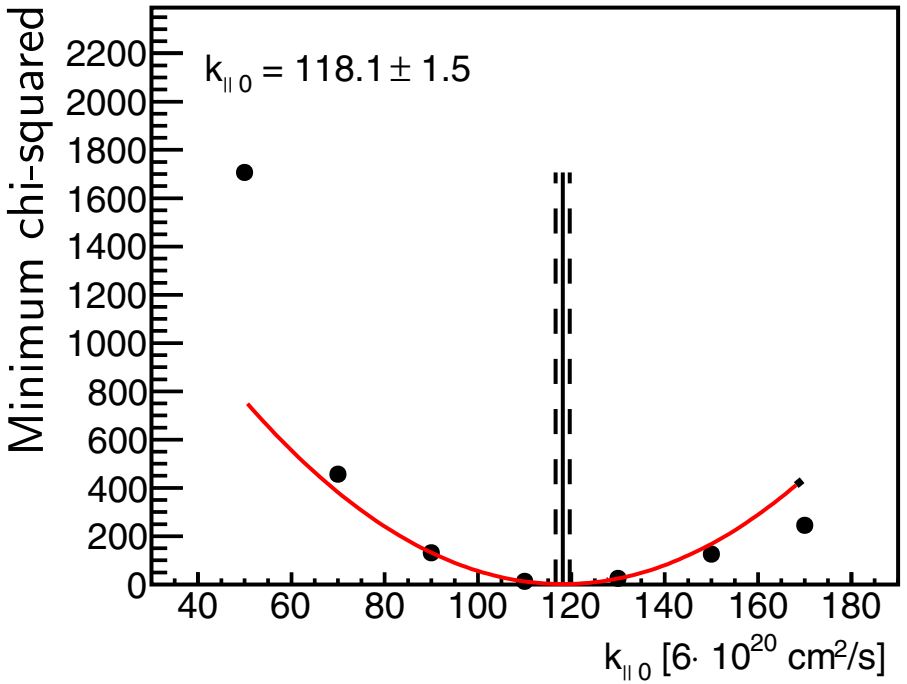

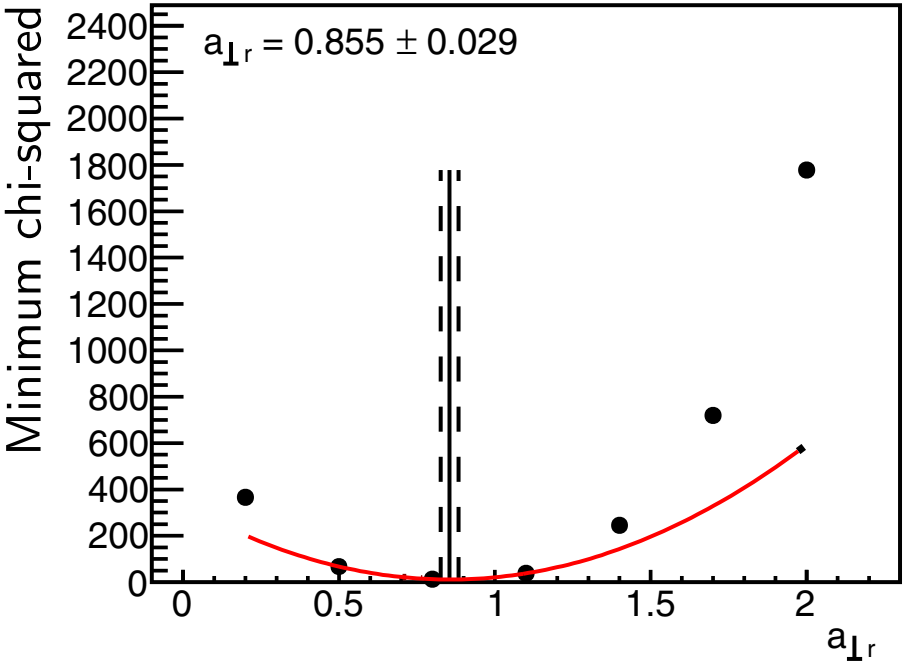

Fit results: DC normalization

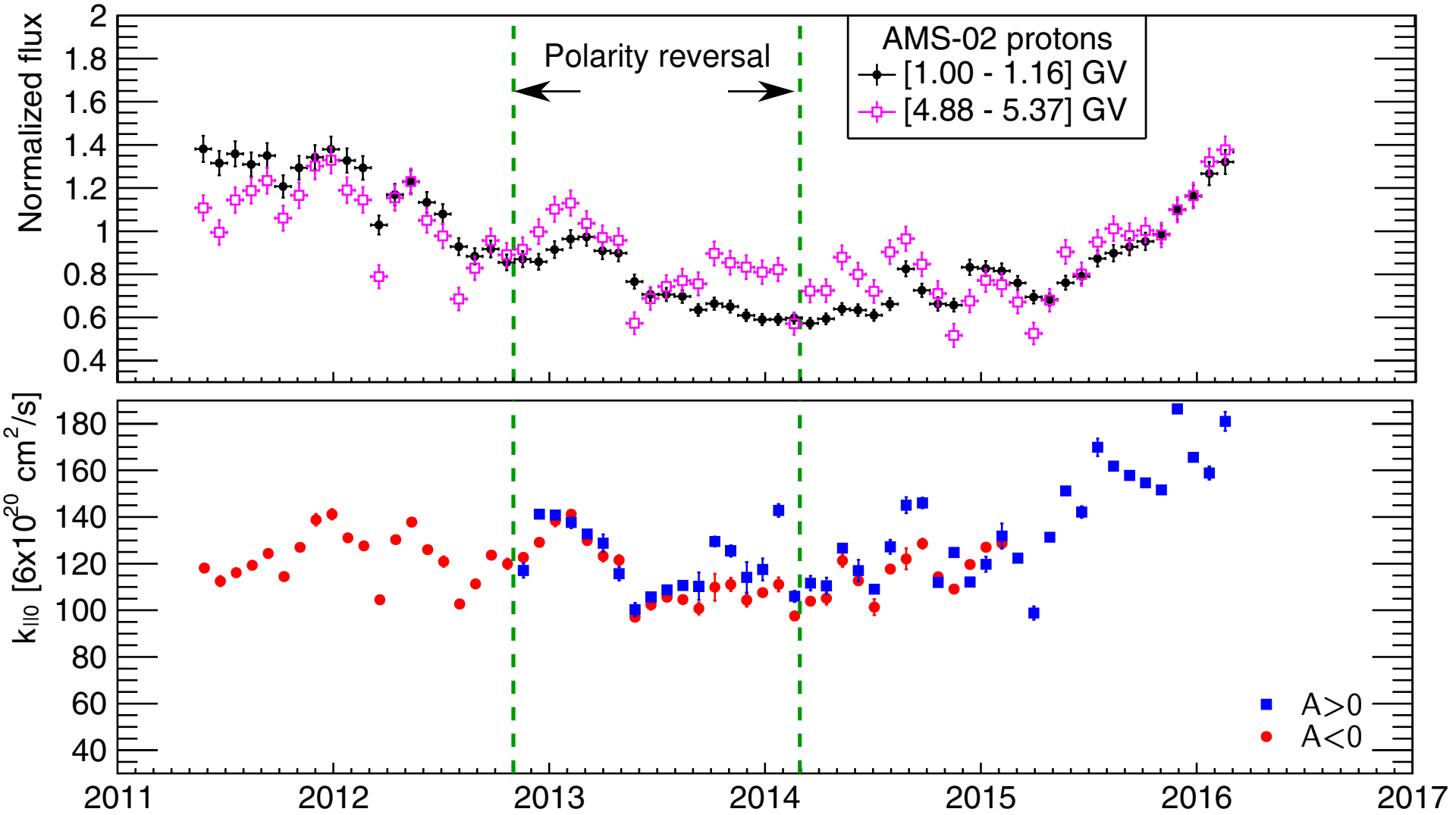

Fit results: DC normalization

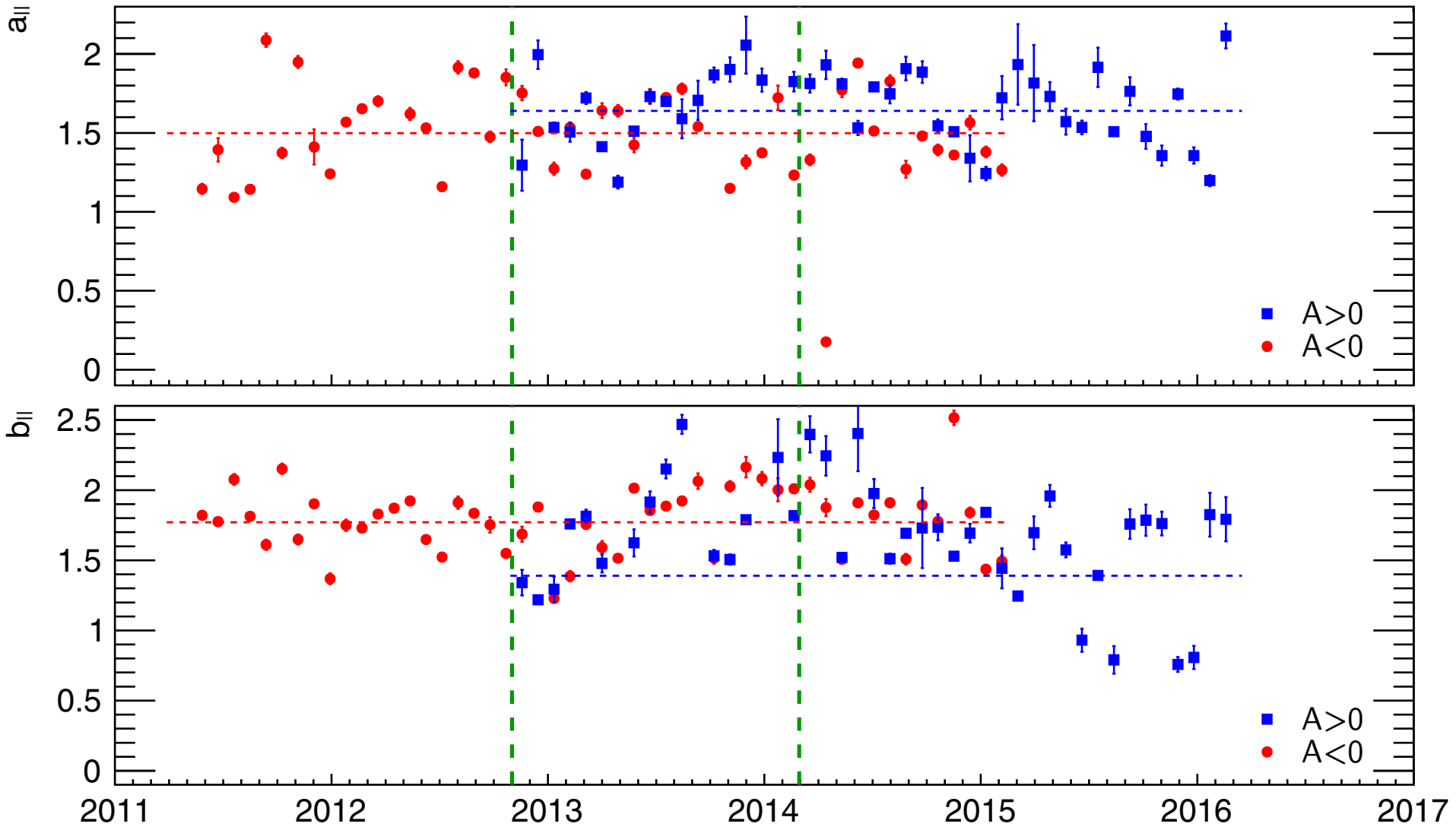

Fit results: perpendicular DC slopes

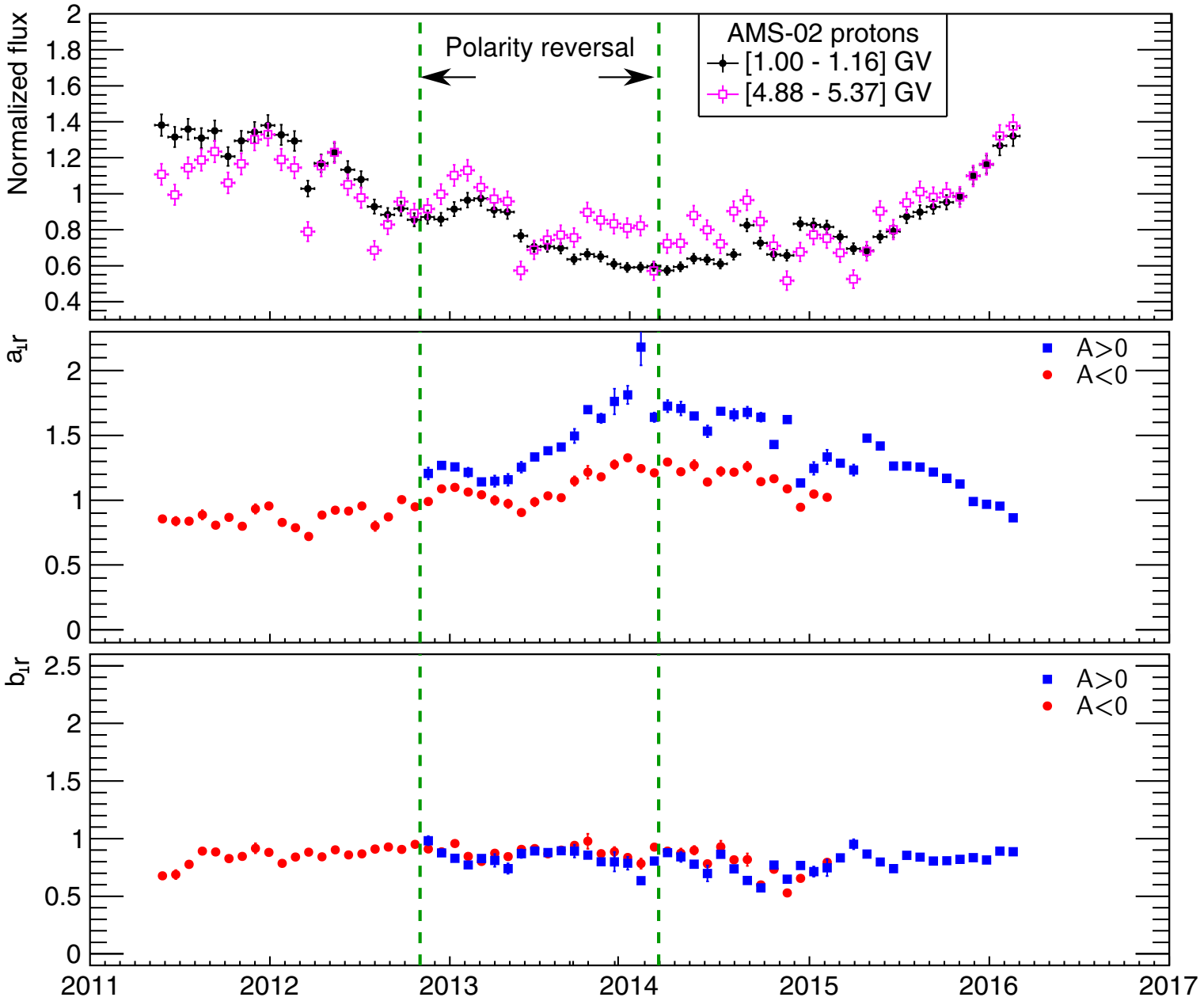

From AMS-02 to Mars

For each AMS-02 monthly flux, the best-fit model is used to compute the modulated flux in the average Mars position of the given month.

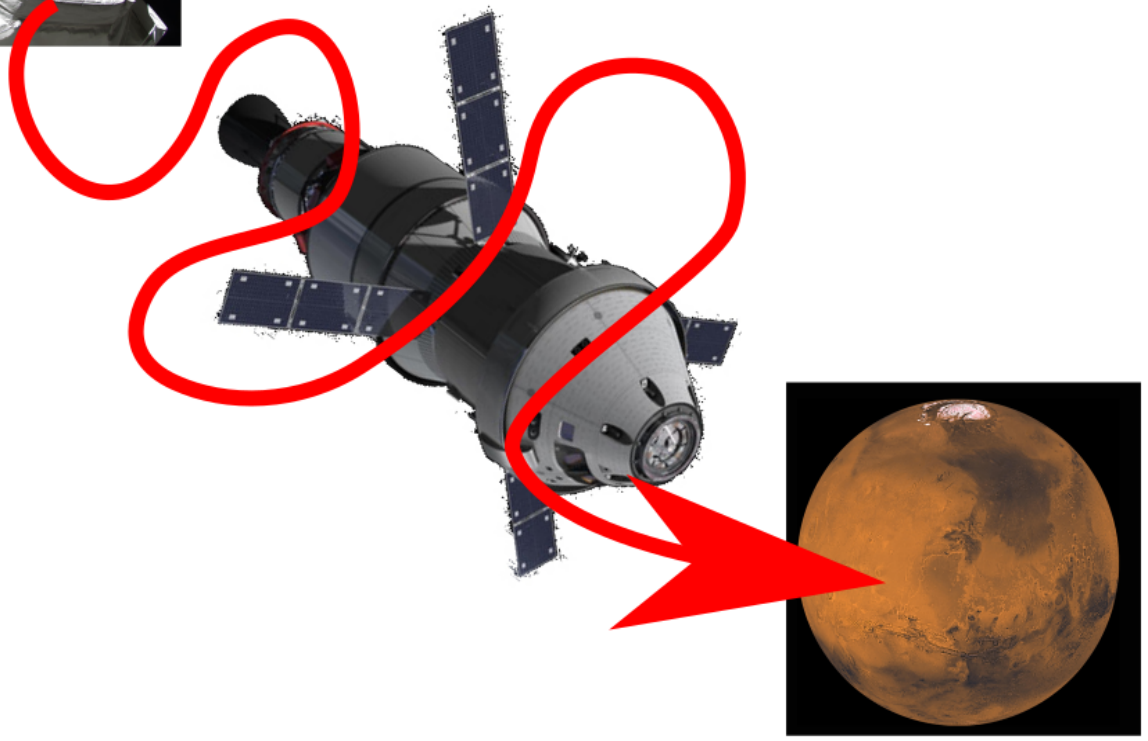

Mars-to-Earth flux ratio

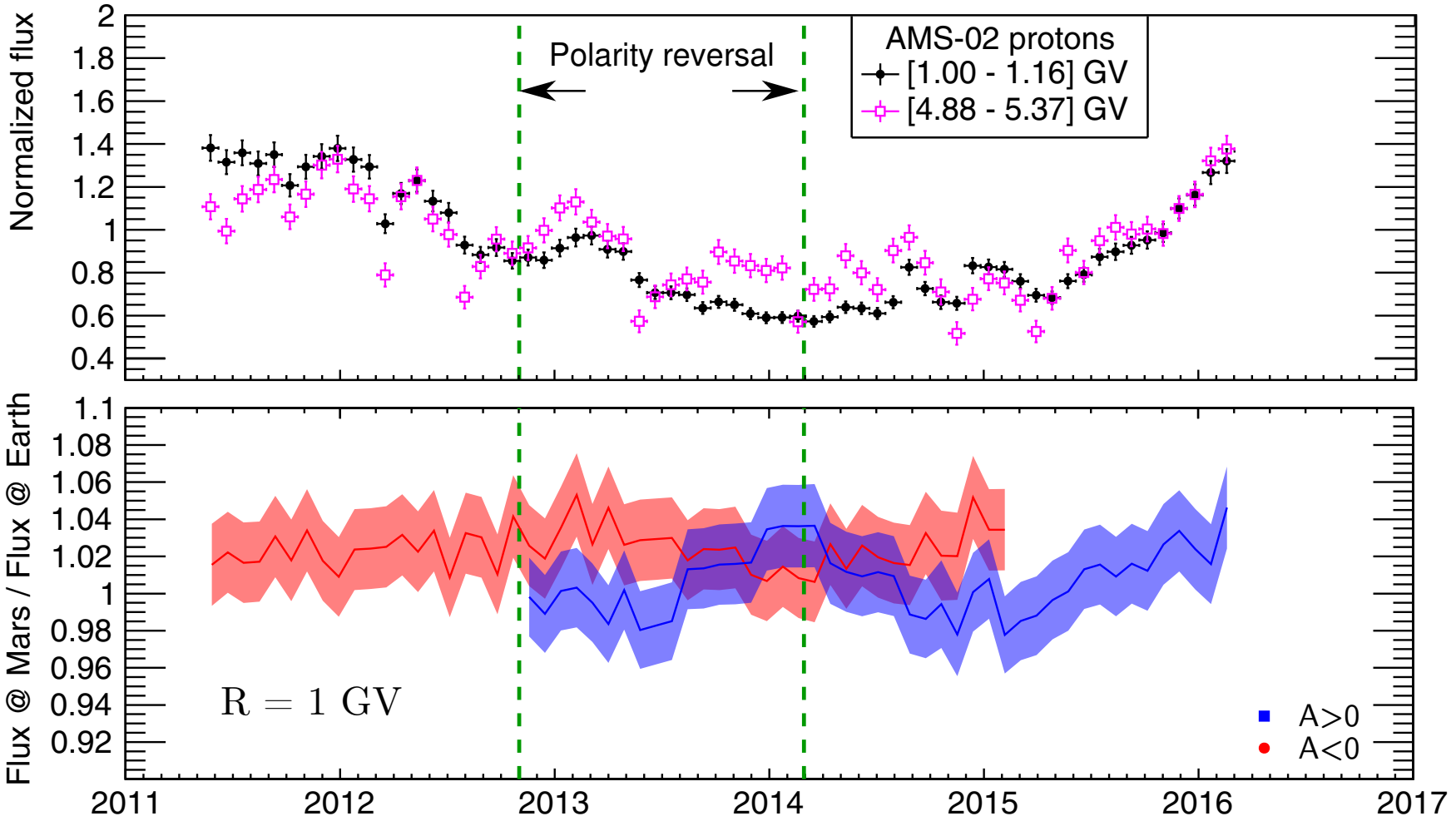

Conclusions

- A new parametrization of the proton and helium LIS has been derived from the latest data of Voyager 1 and AMS-02
- A three-dimensional numerical model for solving the Parker equation has been tuned to match the AMS-02 proton monthly fluxes during the maximum of solar cycle 24
- The normalization of the parallel diffusion coefficient is highly correlated with the short-term structures present in the fluxes; the best-fit value does not depend on the magnetic field polarity
- The slopes of the parallel diffusion coefficient are not constrained by fitting AMS-02 data
- The behavior of the fluxes below and above few GV is driven by the low- and high- rigidity slope of the perpendicular diffusion coefficient; the best-fit value of the low rigidity slope depends on the magnetic field polarity

Backup

Computing time

- Solar wind speed, HMF, diffusion tensor, current sheet and all the needed derivatives are calculated at all grid positions with parallel code on GPU/CPU: $\simeq 30\%$ of the computing time.
- The solution is computed sequentially for each rigidity step (starting from the highest) and for each grid position: $\simeq 70\%$ of the computing time.
  - The rigidity loop cannot be parallelized, because the solution at step `i` is needed for computing the solution at step `i+1`
- Running time:
  - GPU $\simeq 45$s, 1 desktop: $\simeq 1.9$k models/day
  - CPU (6 threads) $\simeq 3$m, CERN batch: $\simeq 80$k models/day

Model instability

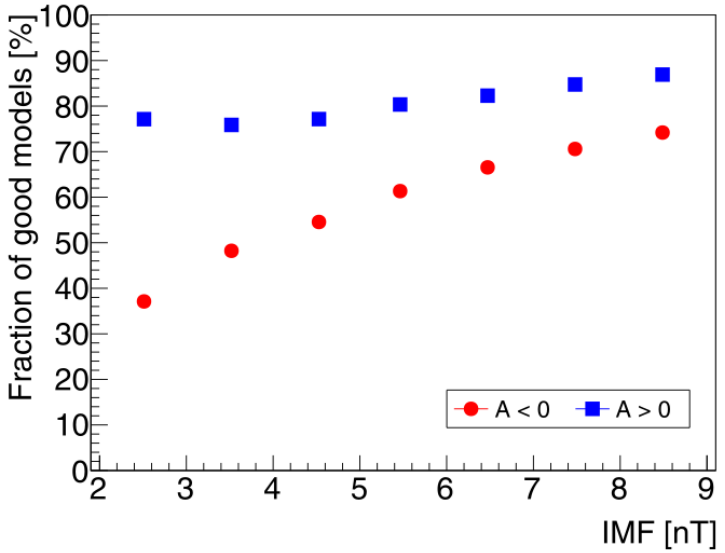

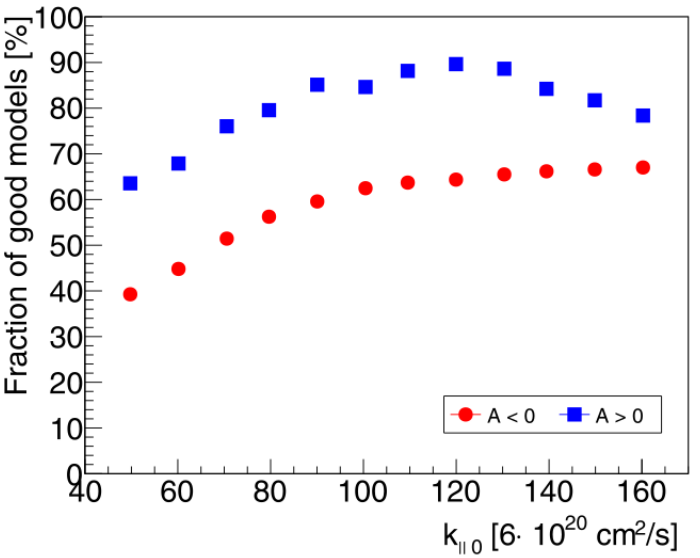

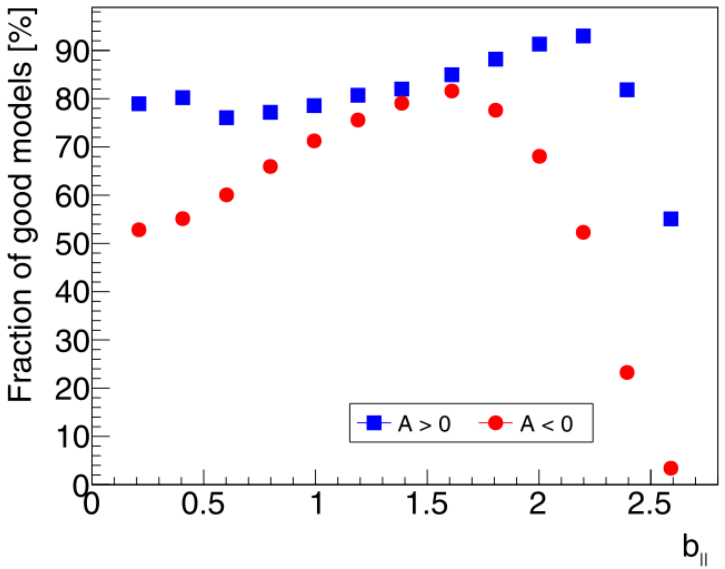

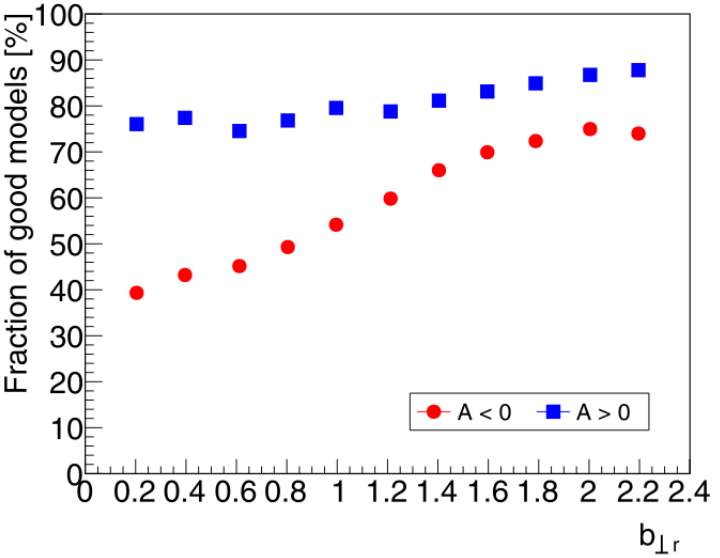

LIS: high energy

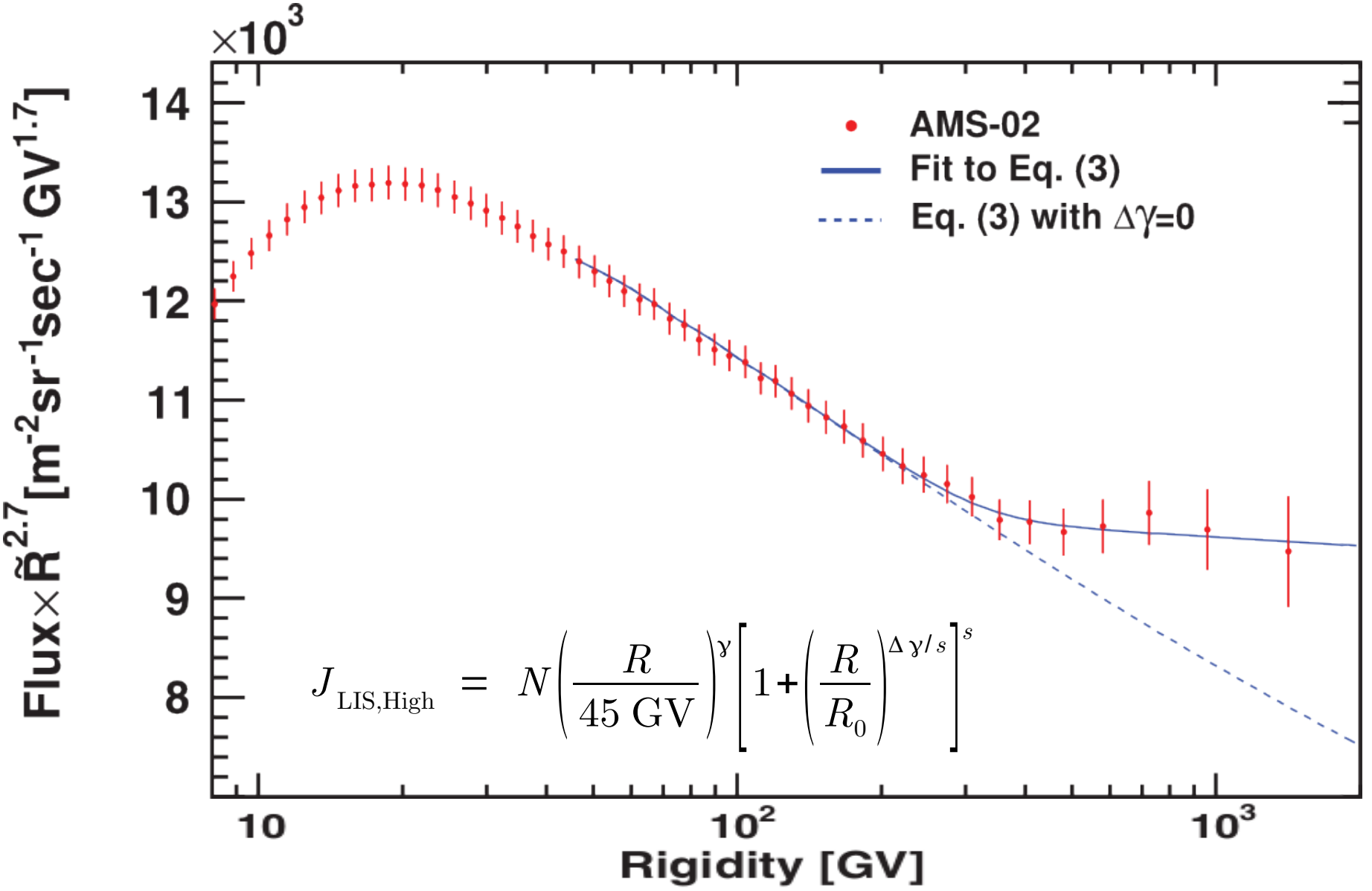

LIS: intermediate energy

Low-energy break found in analysis of Fermi gamma-ray emission in giant molecular clusters

(Neronov et al, 2012, PRL 108)

Three power laws above few GVs:

$$R^{\gamma_1}\left\{1+\left[\frac{R}{R_{b1}}\left(1+\left(\frac{R}{R_{b2}}\right)^{\frac{\Delta\gamma_2}{s_2}}\right)^{s_2}\right]^{\frac{\Delta\gamma_1}{s_1}}\right\}^{s_1}$$

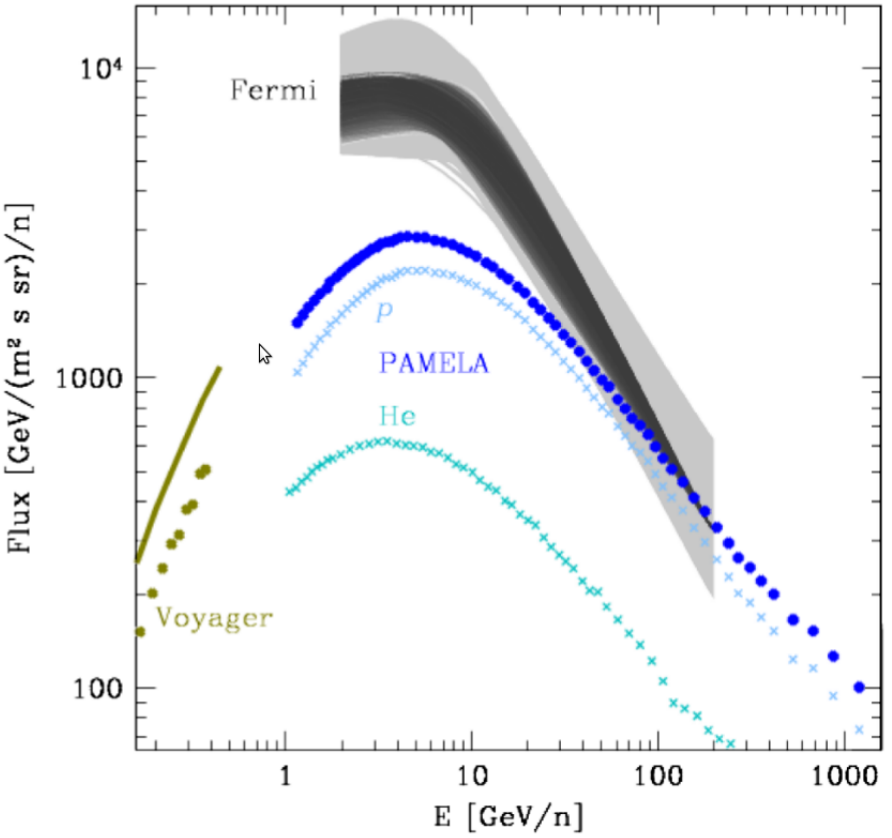

LIS: low energy

Voyager 1 data divided by a power law look like a sigmoid function in log R

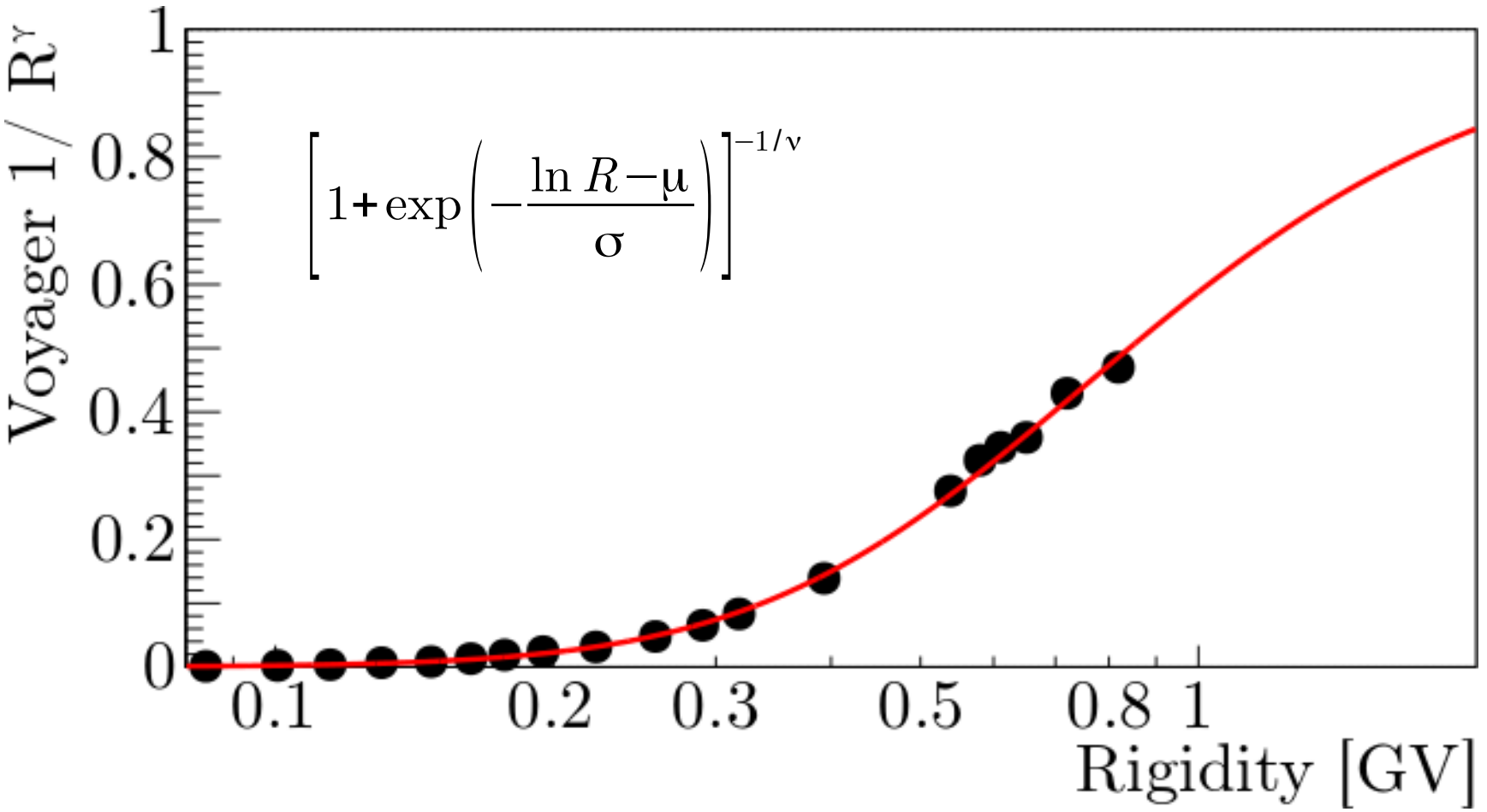

Force-field approximation

- Force-field equation: $\frac{3k_1(r)}{V(r)}\frac{\partial f}{\partial r} + \frac{R}{\beta k_2(R)}\frac{\partial f}{\partial R} = 0$
- Solution: $f(r_E, R_E) = f(r_{HP}, R_{HP}) \Longrightarrow \frac{J(r_E, T_E)}{T_E(T_E+2M)} = \frac{J(r_{HP}, T_{HP})}{T_{HP}(T_{HP}+2M)}$

$$\int_{r_E}^{r_{HP}} \frac{V(r)}{3k_1(r)} dr = \phi = \int_{R_E}^{R_{HP}} \beta \frac{k_2(R)}{R} dR$$

- Diffusion coefficient approximation: $k_2(R) \propto R$

$$\phi = \int_{R_E}^{R_{HP}} \beta \frac{R}{R} dR = \int_{R_E}^{R_{HP}} \frac{1}{Z}\frac{dT}{dR} dR = \frac{T_{HP} - T_E}{Z}$$

$$J(r_E, T_E) = \frac{T_E(T_E+2M)}{(T_E+Z\phi)(T_E+Z\phi+2M)} J(r_{HP}, T_E+Z\phi)$$

Realistic diffusion coefficient

- Generic power-law: $k_2(R) \propto R^{\delta}$
- Solution: $$\phi = \int_{R_E}^{R_{HP}} \beta \frac{R^{\delta}}{R} dR = \int_{R_E}^{R_{HP}} \frac{1}{Z} \frac{R^{\delta}}{\sqrt{R^2+M^2}} dR =$$
$$\frac{1}{ZM(\delta+1)} \left[R_{HP}^{\delta+1} \, {}_2F_1\left(\frac{1}{2}, \frac{a+1}{2}; \frac{a+3}{2}; -\frac{R_{HP}^2}{M^2}\right) - R_E^{\delta+1} \, {}_2F_1\left(\frac{1}{2}, \frac{a+1}{2}; \frac{a+3}{2}; -\frac{R_E^2}{M^2}\right) \right]$$
- There is no analytical solution

Modified force-field approximation

Use two modulation potentials at different rigidities with a transition in between:

$$\phi(R) = \begin{cases} \phi_L & R < R_L \\ f(R, \phi_L, \phi_H) & R_L < R < R_H \\ \phi_H & R > R_H \end{cases}$$

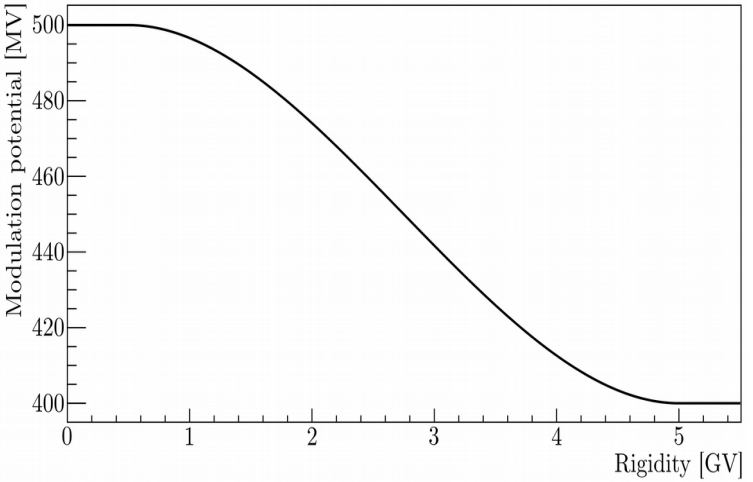

$f =$ smooth function with zero derivative at R_L and $R_H = \phi_L + (\phi_H - \phi_L)\, r^2 (3 - 2\, r)$, where

$$r = \frac{R - R_L}{R_H - R_L}$$

See also Gieseler et al (ICRC2015)

Cross-check on PAMELA data

Force-field approximation

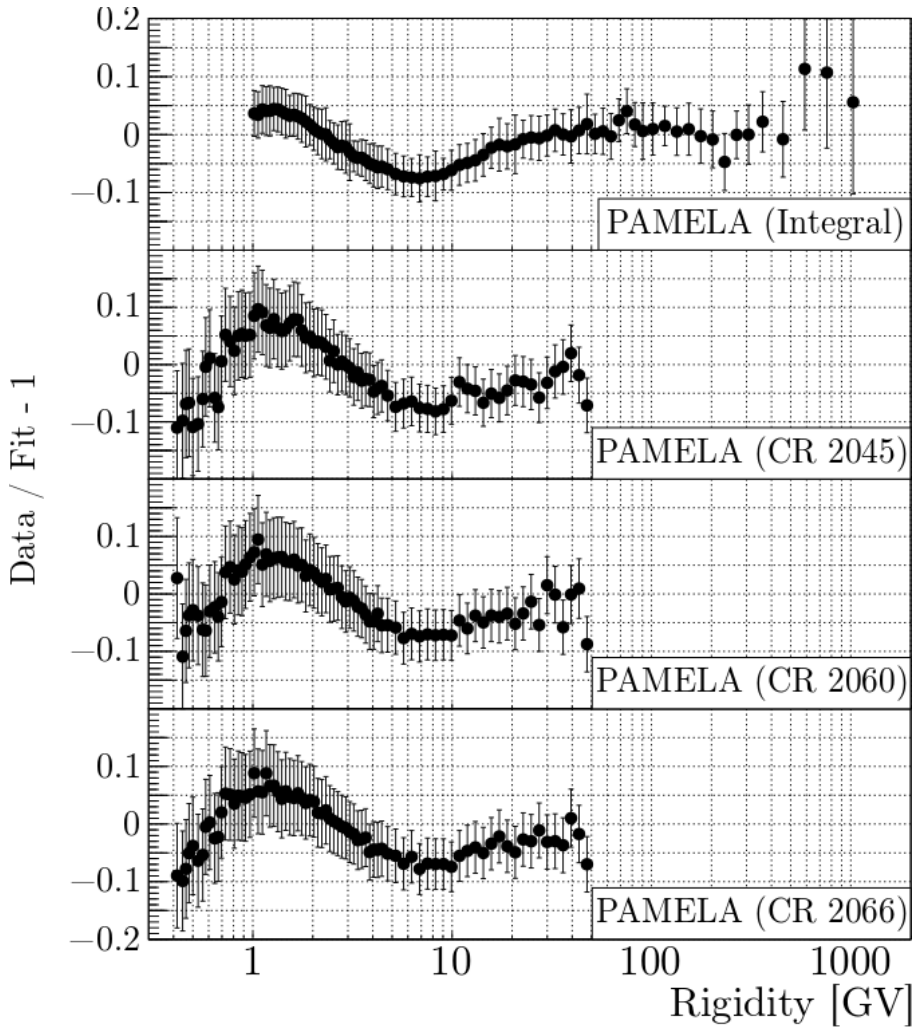

Rigidity-dependent
force-field approximation

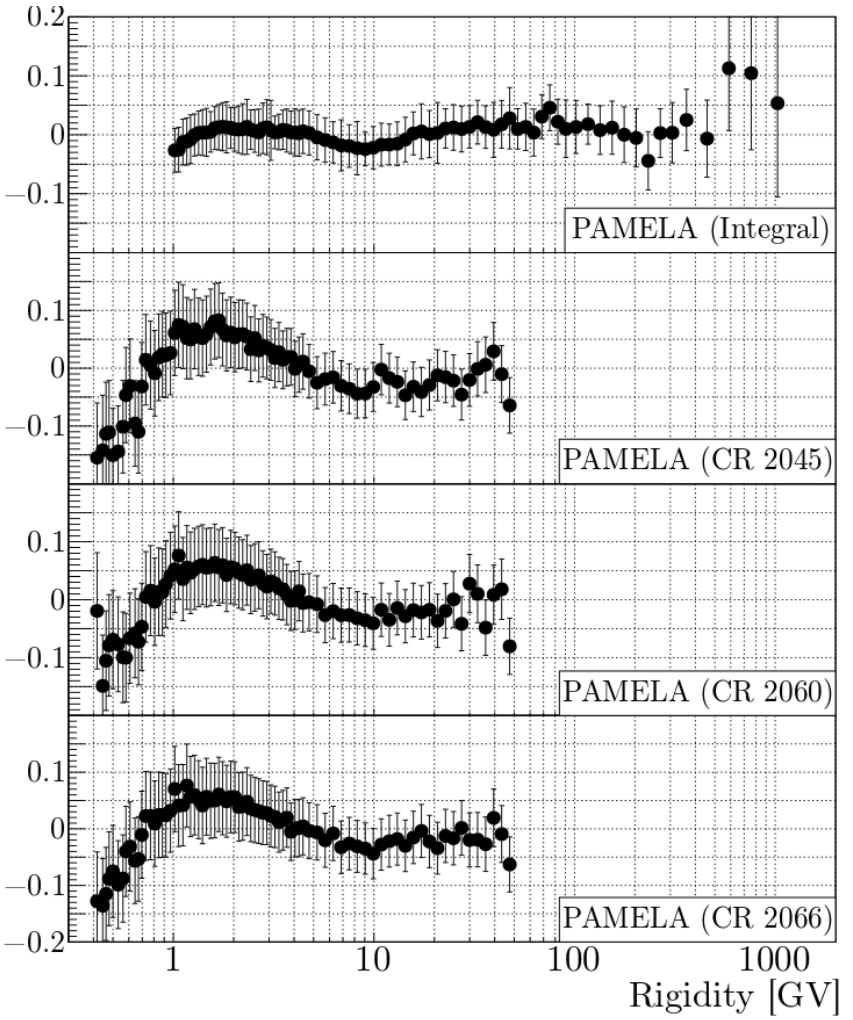

Modulation potentials - PAMELA

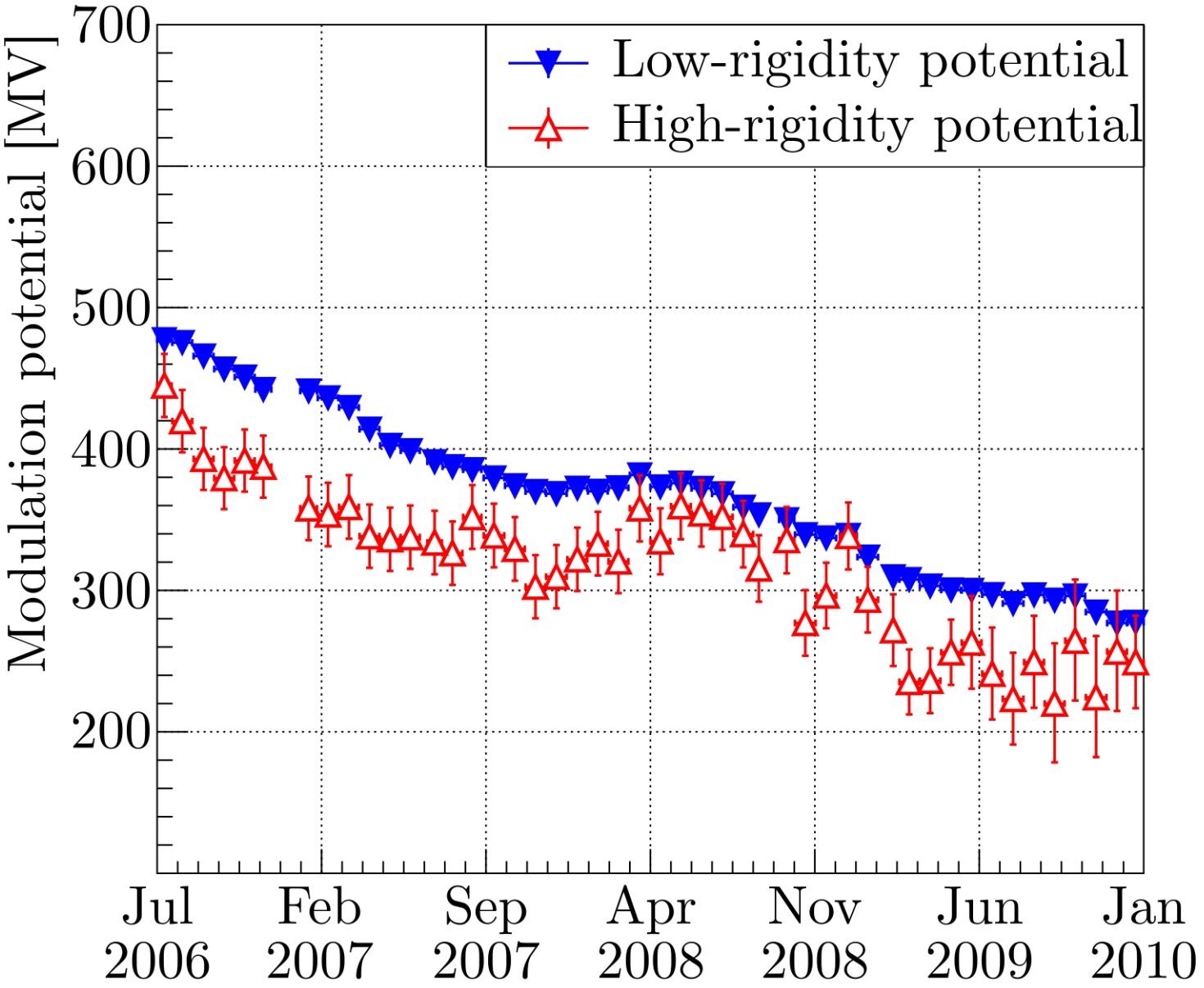

Helium LIS fit result

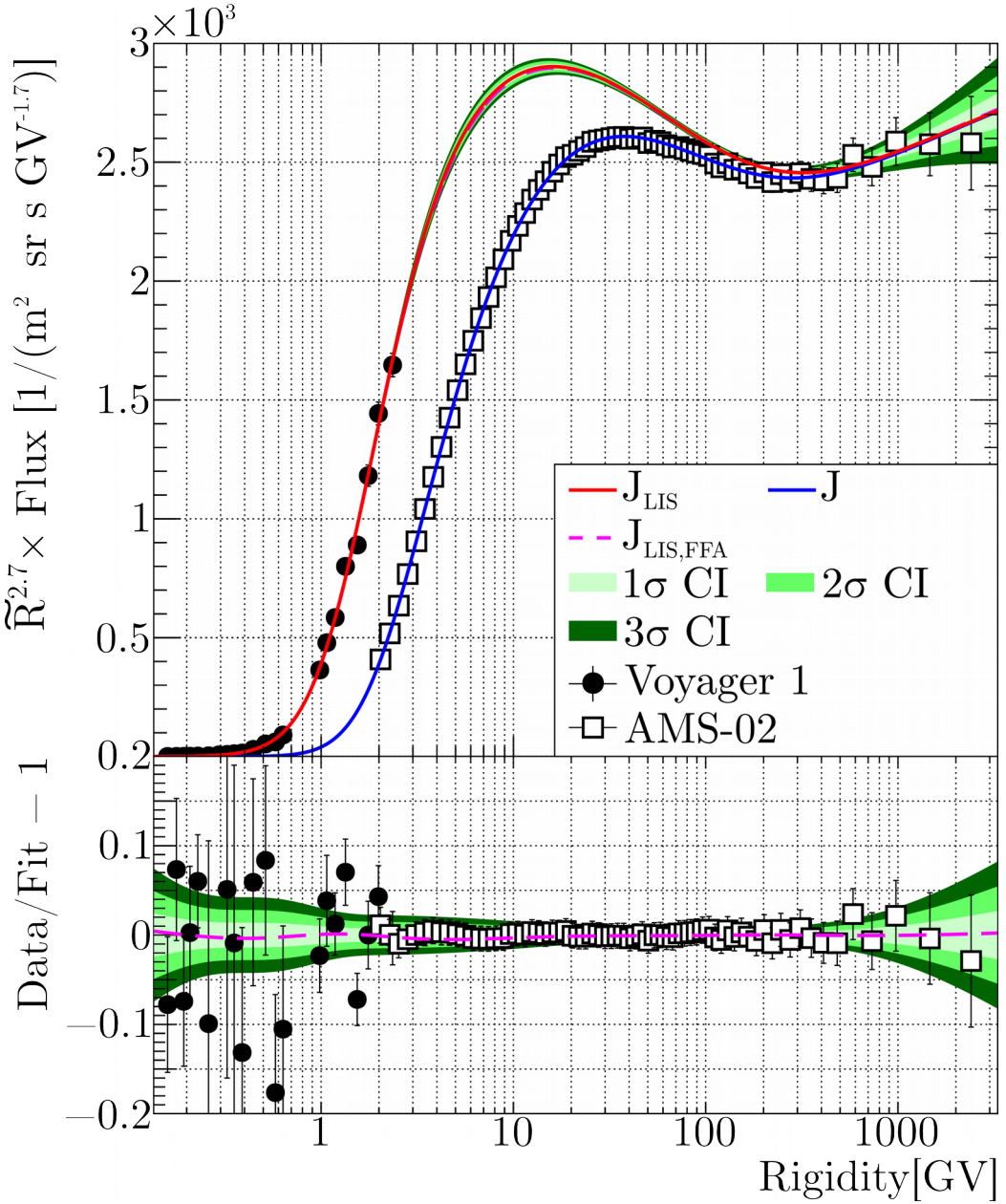

$$\gamma_1 = -1.946 \pm 0.006$$
$$\gamma_2 = -2.7869 \pm 0.0006$$
$$\gamma_3 = -2.64 \pm 0.20$$

$$R_\mu = (1.22 \pm 0.03)\ \mathrm{GV}$$
$$R_{b1} = (1.79 \pm 0.04)\ \mathrm{GV}$$
$$R_{b2} = (190 \pm 30)\ \mathrm{GV}$$

p/He vs time

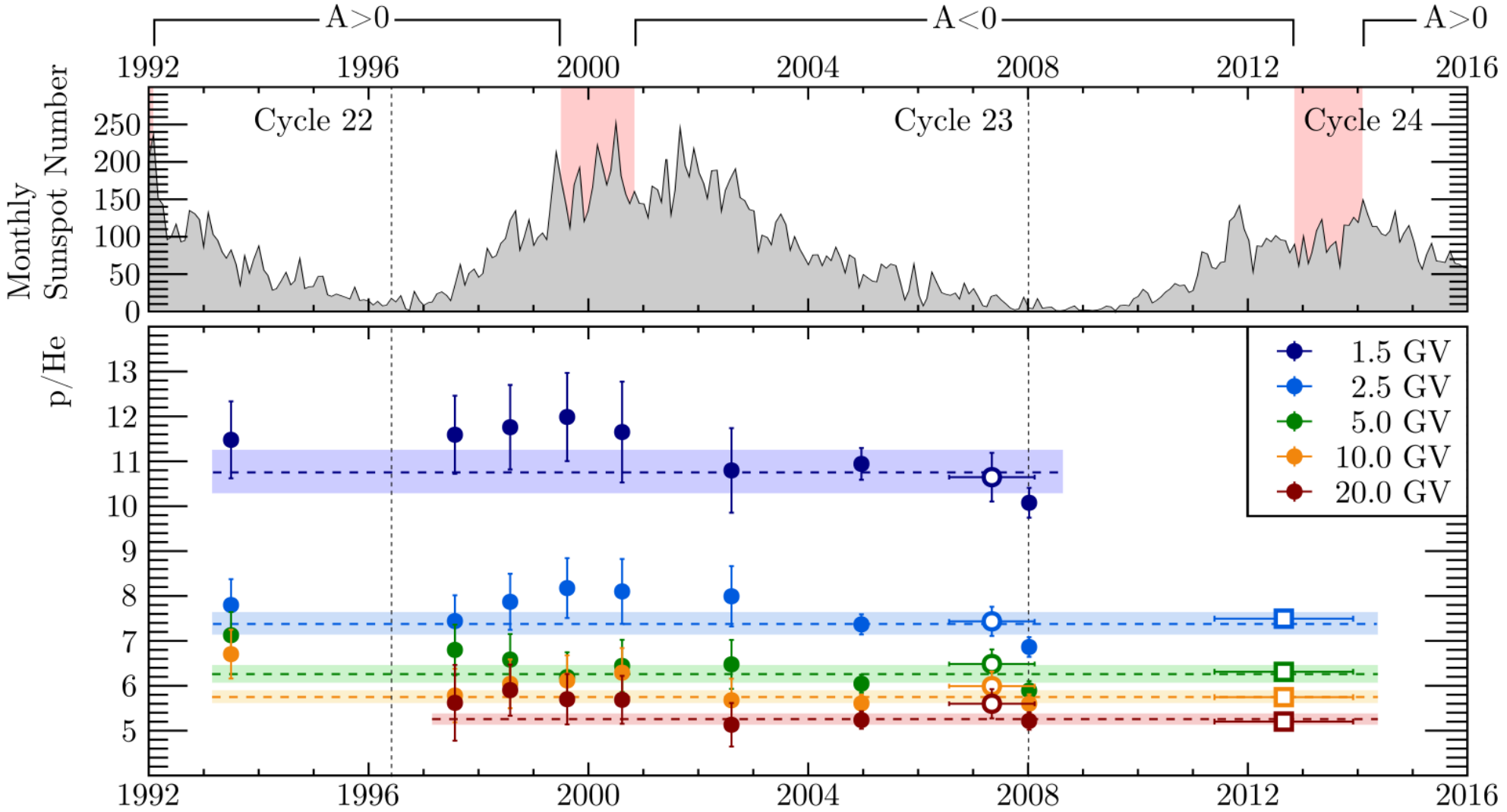
A>0
A<0
A>0
1992
1996
2000
2004
2008
2012
2016
Cycle 22
Cycle 23
Cycle 24
Monthly Sunspot Number
250
200
150
100
50
0
p/He
13
12
11
10
9
8
7
6
5
1.5 GV
2.5 GV
5.0 GV
10.0 GV
20.0 GV

Modulation of p and He

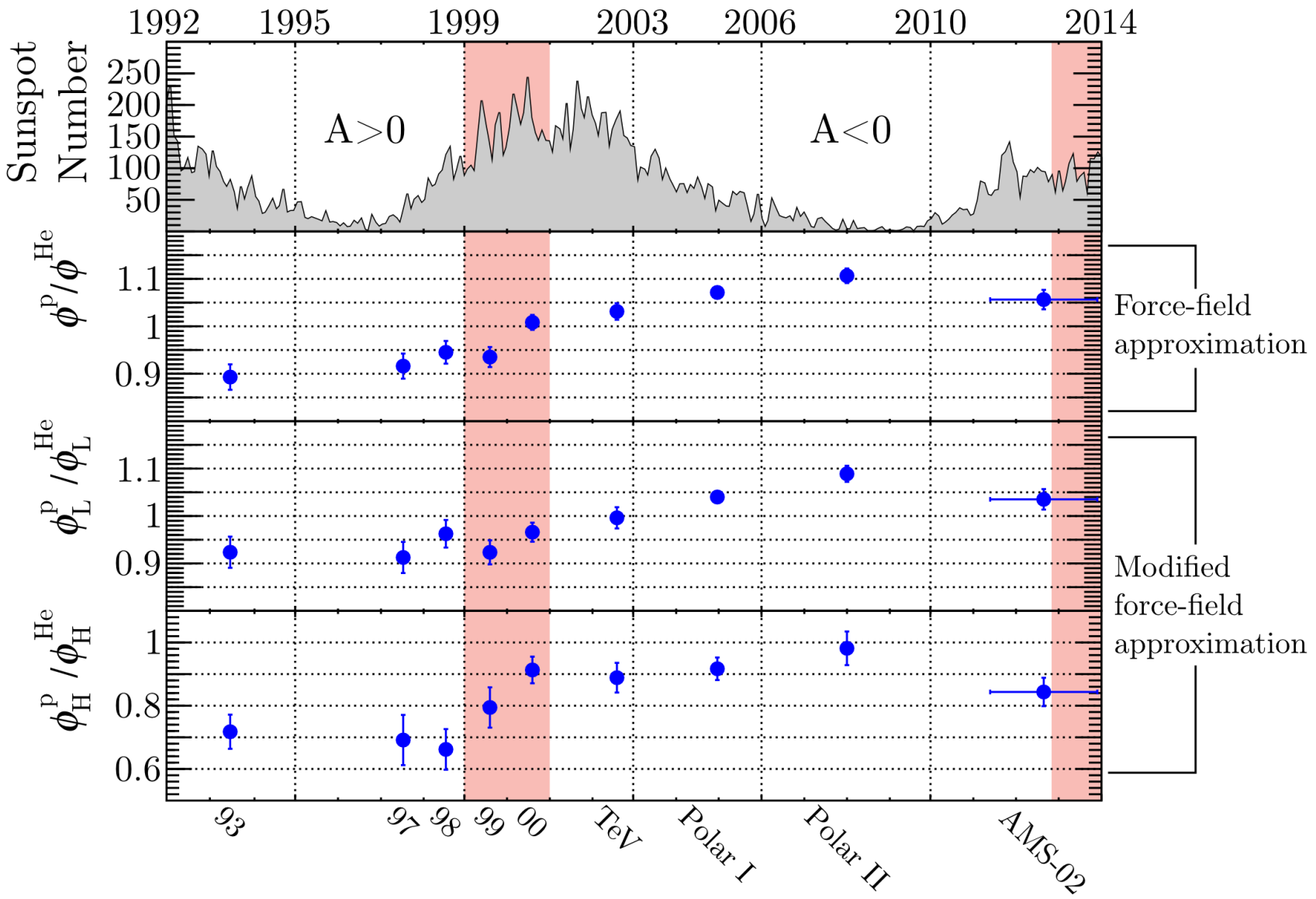

More details: Corti et al, 2016, ApJ, 892, 8

LIS comparison

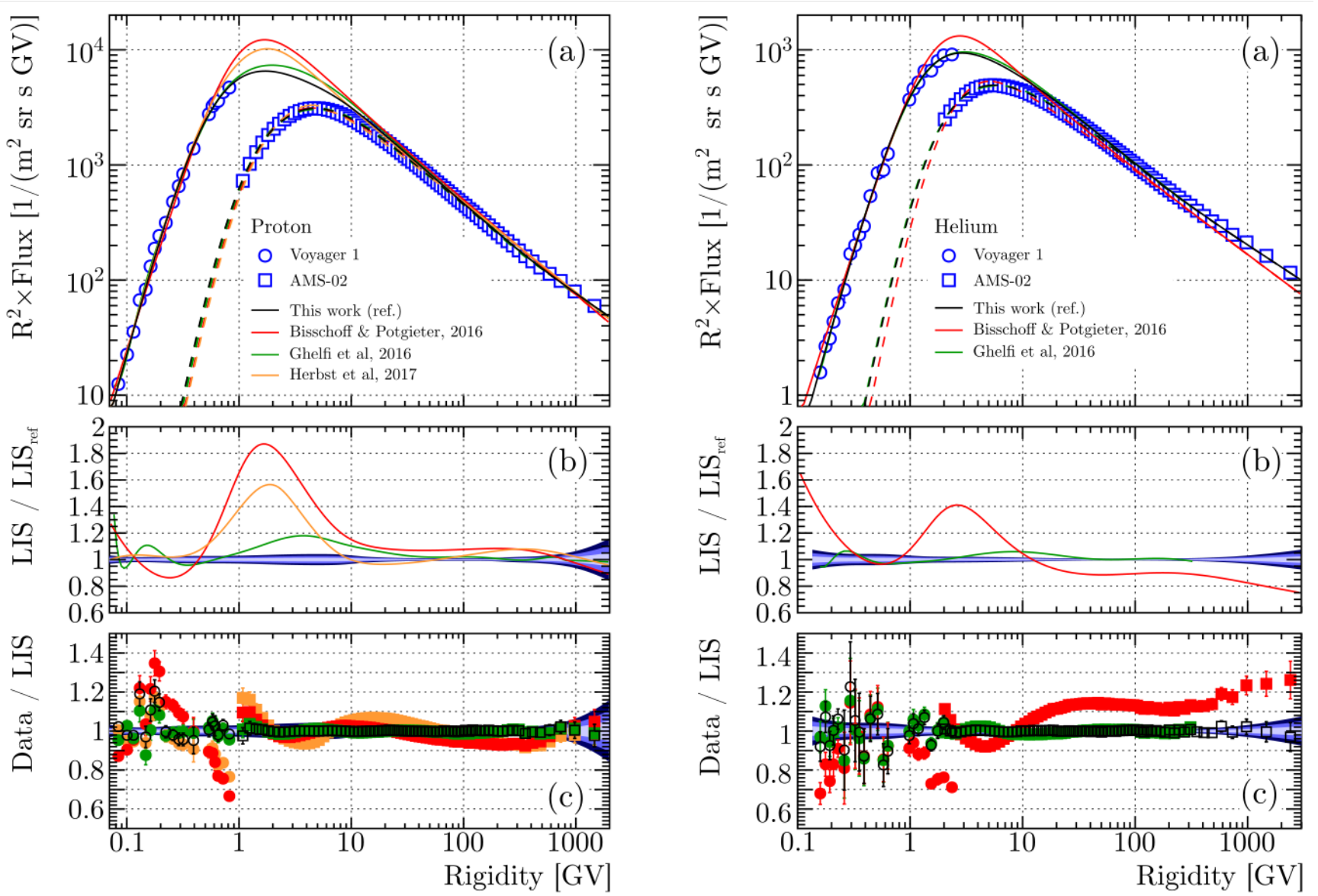

Modulation potentials – AMS-02

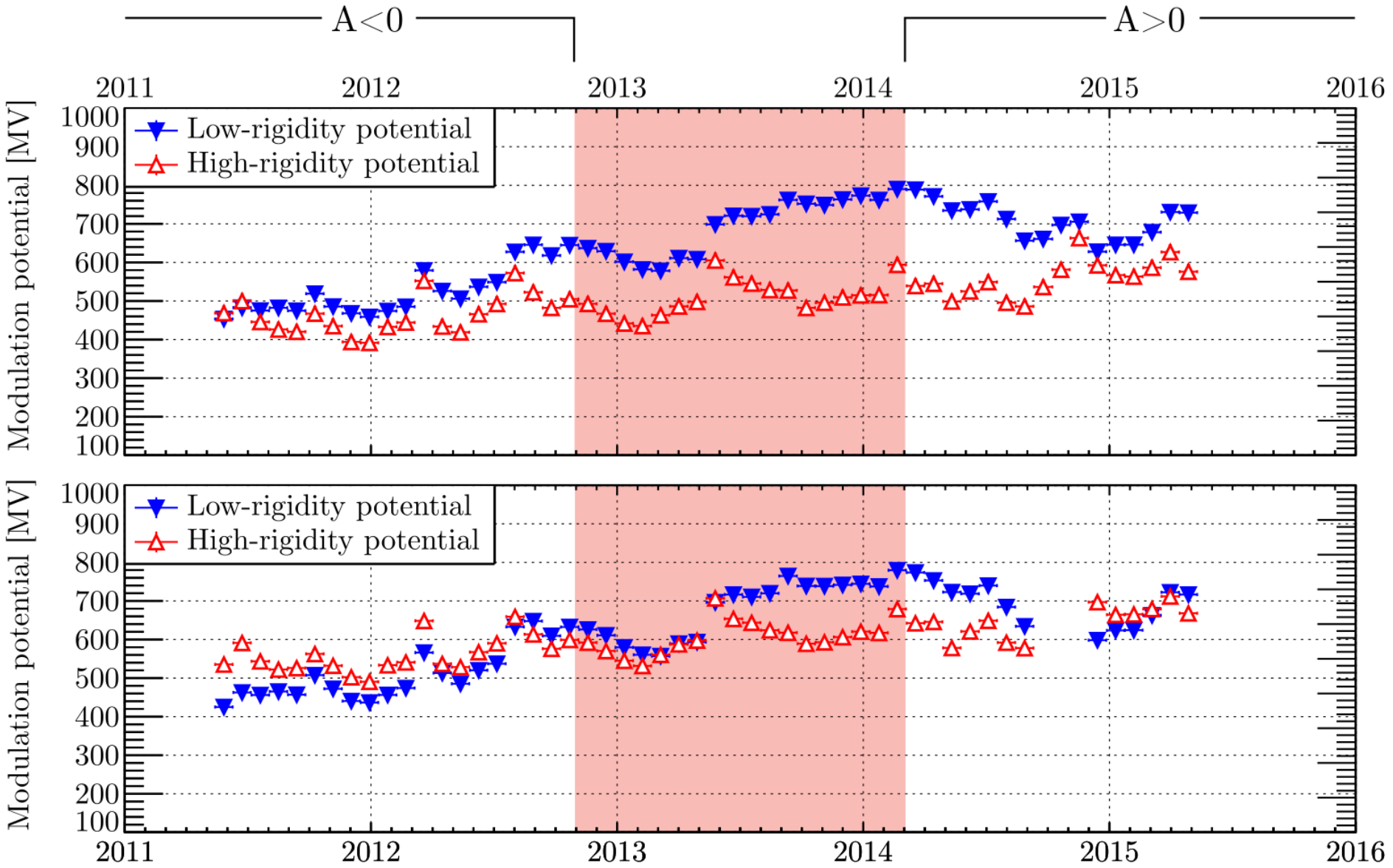

Modulation of p and He with AMS-02